

Probing new physics in semileptonic Λ_b decays

Atasi Ray^{a,*}, Suchismita Sahoo^{b,†} and Rukmani Mohanta^{a,‡}

^a*School of Physics, University of Hyderabad, Hyderabad-500046, India*

^b*Theoretical Physics Division, Physical Research Laboratory, Ahmedabad-380009, India*

Abstract

In recent times, several hints of lepton non-universality have been observed in semileptonic B meson decays, both in the charged-current ($b \rightarrow cl\bar{\nu}_l$) and neutral-current ($b \rightarrow sll$) transitions. Motivated by these intriguing results, we perform a model independent analysis of the semileptonic Λ_b decays involving the quark level transitions $b \rightarrow (u, c)l\nu_l$, in order to scrutinize the nature of new physics. We constrain the new parameter space by using the measured branching ratios of $B_{c,u}^+ \rightarrow \tau^+\nu_\tau$, $B \rightarrow \pi\tau\nu_\tau$ processes and the existing experimental results on $R_{D^{(*)}}$, $R_{J/\psi}$ and R_π^l parameters. Using the constrained parameters, we estimate the branching ratios, forward backward asymmetries, hadron and lepton polarization asymmetries of the $\Lambda_b \rightarrow (\Lambda_c, p)l\nu_l$ processes. Moreover, we also examine whether there could be any lepton universality violation in these decay modes.

*Electronic address: atasiray92@gmail.com

†Electronic address: suchismita8792@gmail.com

‡Electronic address: rmsp@uohyd.ernet.in

I. INTRODUCTION

Though the Standard Model (SM) is considered as the most fundamental theory describing almost all the phenomena of particle physics, still it is unable to shed light on some of the open issues, like matter-antimatter asymmetry, dark matter, dark energy, etc., which eventually necessitates to probe the physics beyond it. In this respect, the rare decays of B mesons involving the flavor changing neutral current (FCNC) transitions play an important role in the quest for new physics (NP). Even though the SM gauge interactions are lepton flavor universal, the violation of lepton universality has been observed in various semileptonic B decays. Recently, the LHCb Collaboration has reported a spectacular discrepancy of 1.9σ (3.3σ) [1–6] and 2σ [7] on the lepton non-universality (LNU) parameters $R_{D^{(*)}} = \text{Br}(\bar{B} \rightarrow \bar{D}^{(*)}\tau\bar{\nu}_\tau)/\text{Br}(\bar{B} \rightarrow \bar{D}^{(*)}l\bar{\nu}_l)$ and $R_{J/\psi} = \text{Br}(B_c \rightarrow J/\psi\tau\bar{\nu}_\tau)/\text{Br}(B_c \rightarrow J/\psi l\bar{\nu}_l)$ respectively from their corresponding SM values. Analogous LNU parameters are also observed in $b \rightarrow sll$ processes i.e., $R_{K^{(*)}} = \text{Br}(\bar{B} \rightarrow \bar{K}^{(*)}\mu^+\mu^-)/\text{Br}(\bar{B} \rightarrow \bar{K}^{(*)}e^+e^-)$ with discrepancies of 2.6σ ($2.2 - 2.4$) σ [8, 9]. The SM predictions as well as the corresponding experimental values of various LNU parameters along with their deviations are presented in Table I.

TABLE I: List of measured lepton non-universality parameters.

| LNU parameters | Experimental value | SM prediction | Deviation |
|---|---|----------------------------|-------------|
| $R_K _{q^2 \in [1,6] \text{ GeV}^2}$ | $0.745^{+0.090}_{-0.074} \pm 0.036$ [8] | 1.003 ± 0.0001 [10] | 2.6σ |
| $R_{K^*} _{q^2 \in [0.045, 1.1] \text{ GeV}^2}$ | $0.66^{+0.11}_{-0.07} \pm 0.03$ [9] | 0.92 ± 0.02 [11] | 2.2σ |
| $R_{K^*} _{q^2 \in [1.1, 6] \text{ GeV}^2}$ | $0.69^{+0.11}_{-0.07} \pm 0.05$ [9] | 1.00 ± 0.01 [11] | 2.4σ |
| R_D | $0.391 \pm 0.041 \pm 0.028$ [6] | 0.300 ± 0.008 [12] | 1.9σ |
| R_{D^*} | $0.316 \pm 0.016 \pm 0.010$ [6] | 0.252 ± 0.003 [13, 14] | 3.3σ |
| $R_{J/\psi}$ | $0.71 \pm 0.17 \pm 0.184$ [7] | 0.289 ± 0.01 [15, 16] | 2σ |

In addition, another discrepancy in $b \rightarrow ul\bar{\nu}_l$ transition is also noticed in the measured ratio

$$R_\pi^l = \frac{\tau_{B^0}}{\tau_{B^-}} \frac{\text{Br}(B^- \rightarrow \tau^- \bar{\nu}_\tau)}{\text{Br}(B^0 \rightarrow \pi^+ l^- \bar{\nu}_l)}, \quad l = e, \mu, \quad (1)$$

where τ_{B^0} (τ_{B^-}) is the life time of B^0 (B^-) meson. Using the experimental measured values

of the branching ratios of $B_u^- \rightarrow \tau^- \bar{\nu}_\tau$ and $B^0 \rightarrow \pi^+ l^- \bar{\nu}_l$ decay processes

$$\text{Br}(B_u^- \rightarrow \tau^- \bar{\nu}_\tau)|^{\text{Expt}} = (1.09 \pm 0.24) \times 10^{-4}, \quad (2)$$

$$\text{Br}(B^0 \rightarrow \pi^+ l^- \bar{\nu}_l)|^{\text{Expt}} = (1.45 \pm 0.05) \times 10^{-4}, \quad (3)$$

with $\tau_{B^-}/\tau_{B^0} = 1.076 \pm 0.004$ from [17], one can obtain

$$R_\pi^l|^{\text{Expt}} = 0.699 \pm 0.156, \quad (4)$$

which has also nearly 1σ deviation from its SM value $R_\pi^l|^{\text{SM}} = 0.583 \pm 0.055$. It is generally argued that, compared to the first two generations, the processes involving the third generation leptons are more sensitive to NP due to their reasonably large mass. As the LNU parameters are the ratio of branching fractions, the uncertainties arising due to the CKM matrix elements and hadronic form factors are expected to be reduced, as they cancelled out in the ratio. Hence, these deviations of various LNU parameters hint towards the possible interplay of new physics in an ambiguous manner.

On the other hand, around 20% of the total number of hadrons produced at LHCb are Λ_b baryon [18, 19], and hence the study of Λ_b becomes quite interesting in these days. The $b \rightarrow ql\bar{\nu}_l$ ($q = u, c$) quark level transitions can be probed in both B and Λ_b decays. Thus, as in B decays one can also scrutinize the presence of lepton universality violation in the corresponding semileptonic baryon decays $\Lambda_b \rightarrow (\Lambda_c, p)l\bar{\nu}_l$ to corroborate the results from B sector and thus, to probe the structure of NP. The heavy-heavy and heavy-light semileptonic decays of baryons can serve as an additional source for the determination of the Cabbibo-Kobayashi-Maskawa (CKM) matrix elements V_{qb} [17, 20–22]. In the literature [23–35], the baryonic decay modes mediated by $b \rightarrow (u, c)l\bar{\nu}_l$ quark level transitions are studied both in model dependent and independent approaches. The analysis of $\Lambda_b \rightarrow \Lambda_c \tau \bar{\nu}_\tau$ decay in the context of SM and various NP couplings are performed in [25]. In Ref. [27], the SM hadron and lepton polarization asymmetries are computed in the covariant confined quark model. The precise lattice QCD calculation of $\Lambda_b \rightarrow (\Lambda_c, p)$ form factors and the investigation of semileptonic baryonic $b \rightarrow (u, c)l\bar{\nu}_l$ processes are performed in [28]. Ref. [34] investigates the impact of five possible new physics interactions, adopting five different form factors of $\Lambda_b \rightarrow \Lambda_c \tau \bar{\nu}_\tau$ decay mode. Considering various real NP couplings, the differential decay distributions, forward-backward asymmetries and the ratios of branching fractions of these baryonic decay modes are investigated in [29]. In this work, we intend to analyse the effect

of complex new couplings on $\Lambda_b \rightarrow (\Lambda_c, p) l \bar{\nu}_l$ decay processes in a model independent way. The main goal of this work is to check the possible existence of lepton universality violation in baryonic decays. The new coefficients are constrained by using the branching ratios of $B_{u,c} \rightarrow \tau \bar{\nu}_\tau$, $B \rightarrow \pi \tau \bar{\nu}_\tau$ processes and the experimental data on $R_{D^{(*)}}, R_{J/\psi}, R_\pi^l$ ratios. We then compute the branching ratios, forward-backward asymmetries, lepton and hadron polarization asymmetries of these baryonic decay modes. We also check the LNU parameters by using the constrained new couplings. The main difference between our approach and the previous analyses in [25, 32] is that, we investigate the impact of individual complex new couplings on all the angular observables including the lepton and hadron polarization asymmetries. We use the updated experimental limits on $R_{D^{(*)}}, R_\pi^l$ ratios including new $R_{J/\psi}$ parameter to constrain the allowed parameter space.

The outline of our paper is follows. In section II, we present the general effective Lagrangian of $b \rightarrow (u, c) l \bar{\nu}_l$ processes in presence of NP, and the necessary theoretical framework for analysing these processes. The constraints on new parameter space associated with $b \rightarrow (u, c) l \bar{\nu}_l$ transitions are computed from the experimental data on $R_{D^{(*)}}, R_{J/\psi}, R_\pi^l$, $\text{Br}(B_{c,u} \rightarrow \tau \bar{\nu}_\tau)$ and $\text{Br}(B \rightarrow \pi \tau \bar{\nu}_\tau)$ observables in section III. In section IV, we discuss the branching ratios and all the physical angular observables of $\Lambda_b \rightarrow (\Lambda_c, p) l \bar{\nu}_l$ processes. Our findings are summarized in section V.

II. THEORETICAL FRAMEWORK

The most general effective Lagrangian associated with $B_1 \rightarrow B_2 l \bar{\nu}_l$ decay processes, where $B_1 = \Lambda_b$, $B_2 = \Lambda_c, p$ mediated by the quark level transition $b \rightarrow q l \bar{\nu}_l$, ($q = u, c$) is given by [36, 37]

$$\begin{aligned} \mathcal{L}_{\text{eff}} = & -\frac{4 G_F}{\sqrt{2}} V_{qb} \left\{ (1 + V_L) \bar{l}_L \gamma_\mu \nu_L \bar{q}_L \gamma^\mu b_L + V_R \bar{l}_L \gamma_\mu \nu_L \bar{q}_R \gamma^\mu b_R \right. \\ & \left. + S_L \bar{l}_R \nu_L \bar{q}_R b_L + S_R \bar{l}_R \nu_L \bar{q}_L b_R + T_L \bar{l}_R \sigma_{\mu\nu} \nu_L \bar{q}_R \sigma^{\mu\nu} b_L \right\} + \text{h.c.}, \end{aligned} \quad (5)$$

where G_F denotes the Fermi constant, V_{qb} are the CKM matrix elements and $q(l)_{L,R} = P_{L,R} q(l)$ are the chiral quark(lepton) fields with $P_{L,R} = (1 \mp \gamma_5)/2$ as the projection operators. Here $V_{L,R}, S_{L,R}, T_L$ represent the vector, scalar and tensor type NP couplings, which are zero in the SM.

In the presence of NP, the double differential decay distribution for $B_1 \rightarrow B_2 l \bar{\nu}_l$ processes with respect to q^2 and $\cos \theta_l$ (θ_l is the angle between the directions of parent B_1 baryon and the l^- in the dilepton rest frame) is given as [25, 33]

$$\frac{d\Gamma}{dq^2} = N \left(1 - \frac{m_l^2}{q^2}\right)^2 \left[A_1 + \frac{m_l^2}{q^2} A_2 + 2A_3 + \frac{1}{4}A_4 + \frac{4m_l}{\sqrt{q^2}} (A_5 + A_6) + A_7 \right], \quad (6)$$

where

$$\begin{aligned} A_1 &= 2 \sin^2 \theta_l (H_{\frac{1}{2},0}^2 + H_{-\frac{1}{2},0}^2) + (1 - \cos \theta_l)^2 H_{\frac{1}{2},+}^2 + (1 + \cos \theta_l)^2 H_{-\frac{1}{2},-}^2, \\ A_2 &= 2 \cos^2 \theta_l (H_{\frac{1}{2},0}^2 + H_{-\frac{1}{2},0}^2) + \sin^2 \theta_l (H_{\frac{1}{2},+}^2 + H_{-\frac{1}{2},-}^2) + 2(H_{\frac{1}{2},t}^2 + H_{-\frac{1}{2},t}^2) \\ &\quad - 4 \cos \theta_l (H_{\frac{1}{2},0} H_{\frac{1}{2},t} + H_{-\frac{1}{2},0} H_{-\frac{1}{2},t}), \\ A_3 &= H_{\frac{1}{2},0}^{SP^2} + H_{-\frac{1}{2},0}^{SP^2}, \\ A_4 &= \frac{m_l^2}{q^2} \left[2 \sin^2 \theta_l (H_{\frac{1}{2},+,-}^{T^2} + H_{\frac{1}{2},0,t}^{T^2} + H_{-\frac{1}{2},+,-}^{T^2} + H_{-\frac{1}{2},0,t}^{T^2} + 2H_{\frac{1}{2},+,-}^T H_{\frac{1}{2},0,t}^T + 2H_{-\frac{1}{2},+,-}^T H_{-\frac{1}{2},0,t}^T) \right. \\ &\quad + (1 + \cos \theta_l)^2 (H_{-\frac{1}{2},0,-}^{T^2} + H_{-\frac{1}{2},-,t}^{T^2} + 2H_{-\frac{1}{2},0,-}^T H_{-\frac{1}{2},-,t}^T) \\ &\quad + (1 - \cos \theta_l)^2 (H_{\frac{1}{2},+,0}^{T^2} + H_{\frac{1}{2},+,t}^{T^2} + 2H_{\frac{1}{2},+,0}^T H_{\frac{1}{2},+,t}^T) \left. \right] \\ &\quad + 2 \cos^2 \theta_l (H_{\frac{1}{2},+,-}^{T^2} + H_{\frac{1}{2},0,t}^{T^2} + H_{-\frac{1}{2},+,-}^{T^2} + H_{-\frac{1}{2},0,t}^{T^2} + 2H_{\frac{1}{2},+,-}^T H_{\frac{1}{2},0,t}^T + 2H_{-\frac{1}{2},+,-}^T H_{-\frac{1}{2},0,t}^T) \\ &\quad + \sin^2 \theta_l (H_{\frac{1}{2},+,0}^{T^2} + H_{\frac{1}{2},+,t}^{T^2} + H_{-\frac{1}{2},+,0}^{T^2} + H_{-\frac{1}{2},+,t}^{T^2} + 2H_{\frac{1}{2},+,0}^T H_{\frac{1}{2},+,t}^T + 2H_{-\frac{1}{2},+,0}^T H_{-\frac{1}{2},+,t}^T), \\ A_5 &= -\cos \theta_l (H_{\frac{1}{2},0} H_{\frac{1}{2},0}^{SP} + H_{-\frac{1}{2},0} H_{-\frac{1}{2},0}^{SP}) + (H_{\frac{1}{2},t} H_{\frac{1}{2},0}^{SP} + H_{-\frac{1}{2},t} H_{-\frac{1}{2},0}^{SP}), \\ A_6 &= \frac{\cos^2 \theta_l}{2} (H_{\frac{1}{2},0} H_{\frac{1}{2},+,-}^T + H_{\frac{1}{2},0} H_{\frac{1}{2},0,t}^T + H_{-\frac{1}{2},0} H_{-\frac{1}{2},+,-}^T + H_{-\frac{1}{2},0} H_{-\frac{1}{2},0,t}^T) \\ &\quad - \frac{\cos \theta_l}{2} (H_{\frac{1}{2},t} H_{\frac{1}{2},+,-}^T + H_{\frac{1}{2},t} H_{\frac{1}{2},0,t}^T + H_{-\frac{1}{2},t} H_{-\frac{1}{2},+,-}^T + H_{-\frac{1}{2},t} H_{-\frac{1}{2},0,t}^T) \\ &\quad + \frac{(1 - \cos \theta_l)^2}{4} (H_{\frac{1}{2},+} H_{\frac{1}{2},+,0}^T + H_{\frac{1}{2},+} H_{\frac{1}{2},+,t}^T) \\ &\quad + \frac{(1 + \cos \theta_l)^2}{4} (H_{-\frac{1}{2},-} H_{-\frac{1}{2},0,-}^T + H_{-\frac{1}{2},-} H_{-\frac{1}{2},-,t}^T) \\ &\quad + \frac{\sin^2 \theta_l}{4} (H_{\frac{1}{2},+} H_{\frac{1}{2},+,0}^T + H_{\frac{1}{2},+} H_{\frac{1}{2},+,t}^T + H_{-\frac{1}{2},-} H_{-\frac{1}{2},0,-}^T + H_{-\frac{1}{2},-} H_{-\frac{1}{2},-,t}^T \\ &\quad + 2H_{\frac{1}{2},0} H_{\frac{1}{2},+,-}^T + 2H_{\frac{1}{2},0} H_{\frac{1}{2},0,t}^T + 2H_{-\frac{1}{2},0} H_{-\frac{1}{2},+,-}^T + 2H_{-\frac{1}{2},0} H_{-\frac{1}{2},0,t}^T), \\ A_7 &= -2 \cos \theta_l (H_{\frac{1}{2},0}^{SP} H_{\frac{1}{2},+,-}^T + H_{\frac{1}{2},0}^{SP} H_{\frac{1}{2},0,t}^T + H_{-\frac{1}{2},0}^{SP} H_{-\frac{1}{2},+,-}^T + H_{-\frac{1}{2},0}^{SP} H_{-\frac{1}{2},0,t}^T), \end{aligned} \quad (7)$$

with

$$\begin{aligned} H_{\lambda_{\Lambda_c}, \lambda}^{VA} &= H_{\lambda_{\Lambda_c}, \lambda}^V - H_{\lambda_{\Lambda_c}, \lambda}^A, \quad H_{\lambda_{\Lambda_c}, \lambda_w}^V = H_{-\lambda_{\Lambda_c}, -\lambda_w}^V, \quad H_{\lambda_{\Lambda_c}, \lambda_w}^A = -H_{-\lambda_{\Lambda_c}, -\lambda_w}^A, \\ H_{\lambda_{\Lambda_c}, \lambda=0}^{SP} &= H_{\lambda_{\Lambda_c}, \lambda=0}^S + H_{\lambda_{\Lambda_c}, \lambda=0}^P, \quad H_{\lambda_{\Lambda_c}, \lambda_{NP}}^S = H_{-\lambda_{\Lambda_c}, -\lambda_{NP}}^S, \quad H_{\lambda_{\Lambda_c}, \lambda_{NP}}^P = -H_{-\lambda_{\Lambda_c}, -\lambda_{NP}}^P, \\ H_{\lambda_{\Lambda_c}, \lambda, \lambda'}^T &= -H_{\lambda_{\Lambda_c}, \lambda', \lambda}^T, \quad H_{\lambda_{\Lambda_c}, \lambda, \lambda}^T = 0. \end{aligned} \quad (8)$$

and

$$N = \frac{G_F^2 |V_{qb}|^2 q^2 \sqrt{\lambda(M_{B_1}^2, M_{B_2}^2, q^2)}}{2^{10} \pi^3 M_{B_1}^3}, \quad \lambda(a, b, c) = a^2 + b^2 + c^2 - 2(ab + bc + ca). \quad (9)$$

Here $M_{B_{1(2)}}$ and m_l are the masses of $B_{1(2)}$ baryon and charged leptons respectively. The helicity amplitudes in terms of the various form factors and the NP couplings are given as [25, 33]

$$\begin{aligned} H_{\frac{1}{2}0}^V &= (1 + V_L + V_R) \frac{\sqrt{Q_-}}{\sqrt{q^2}} \left[(M_{B_1} + M_{B_2}) f_1(q^2) - q^2 f_2(q^2) \right], \\ H_{\frac{1}{2}0}^A &= (1 + V_L - V_R) \frac{\sqrt{Q_+}}{\sqrt{q^2}} \left[(M_{B_1} - M_{B_2}) g_1(q^2) + q^2 g_2(q^2) \right], \\ H_{\frac{1}{2}+}^V &= (1 + V_L + V_R) \sqrt{2Q_-} \left[-f_1(q^2) + (M_{B_1} + M_{B_2}) f_2(q^2) \right], \\ H_{\frac{1}{2}+}^A &= (1 + V_L - V_R) \sqrt{2Q_+} \left[-g_1(q^2) - (M_{B_1} - M_{B_2}) g_2(q^2) \right], \\ H_{\frac{1}{2}t}^V &= (1 + V_L + V_R) \frac{\sqrt{Q_+}}{\sqrt{q^2}} \left[(M_{B_1} - M_{B_2}) f_1(q^2) + q^2 f_3(q^2) \right], \\ H_{\frac{1}{2}t}^A &= (1 + V_L - V_R) \frac{\sqrt{Q_-}}{\sqrt{q^2}} \left[(M_{B_1} + M_{B_2}) g_1(q^2) - q^2 g_3(q^2) \right], \\ H_{\frac{1}{2}0}^S &= (S_L + S_R) \frac{\sqrt{Q_+}}{m_b - m_q} \left[(M_{B_1} - M_{B_2}) f_1(q^2) + q^2 f_3(q^2) \right], \\ H_{\frac{1}{2}0}^P &= (S_L - S_R) \frac{\sqrt{Q_-}}{m_b + m_q} \left[(M_{B_1} + M_{B_2}) g_1(q^2) - q^2 g_3(q^2) \right], \\ H_{\frac{1}{2},+,0}^T &= -T_L \sqrt{\frac{2}{q^2}} \left(f_T \sqrt{Q_+} (M_{B_1} - M_{B_2}) + g_T \sqrt{Q_-} (M_{B_1} + M_{B_2}) \right), \\ H_{\frac{1}{2},+,-}^T &= -T_L \left(f_T \sqrt{Q_+} + g_T \sqrt{Q_-} \right), \\ H_{\frac{1}{2},+,t}^T &= T_L \left[-\sqrt{\frac{2}{q^2}} \left(f_T \sqrt{Q_-} (M_{B_1} + M_{B_2}) + g_T \sqrt{Q_+} (M_{B_1} - M_{B_2}) \right) \right. \\ &\quad \left. + \sqrt{2q^2} \left(f_T^V \sqrt{Q_-} - g_T^V \sqrt{Q_+} \right) \right], \\ H_{\frac{1}{2},0,t}^T &= T_L \left[-f_T \sqrt{Q_-} - g_T \sqrt{Q_+} + f_T^V \sqrt{Q_-} (M_{B_1} + M_{B_2}) - g_T^V \sqrt{Q_+} (M_{B_1} - M_{B_2}) \right. \\ &\quad \left. + f_T^S \sqrt{Q_-} Q_+ + g_T^S \sqrt{Q_+} Q_- \right], \\ H_{-\frac{1}{2},+,-}^T &= T_L \left[f_T \sqrt{Q_+} - g_T \sqrt{Q_-} \right], \\ H_{-\frac{1}{2},0,-}^T &= T_L \left[\sqrt{\frac{2}{q^2}} \left(f_T \sqrt{Q_+} (M_{B_1} - M_{B_2}) - g_T \sqrt{Q_-} (M_{B_1} + M_{B_2}) \right) \right], \end{aligned}$$

$$\begin{aligned}
H_{-\frac{1}{2},-,t}^T &= T_L \left[-\sqrt{\frac{2}{q^2}} \left(f_T \sqrt{Q_-} (M_{B_1} + M_{B_2}) - g_T \sqrt{Q_+} (M_{B_1} - M_{B_2}) \right) \right. \\
&\quad \left. + \sqrt{2q^2} \left(f_T^V \sqrt{Q_-} + g_T^V \sqrt{Q_+} \right) \right], \\
H_{-\frac{1}{2},0,t}^T &= T_L \left[-f_T \sqrt{Q_-} + g_T \sqrt{Q_+} + f_T^V \sqrt{Q_-} (M_{B_1} + M_{B_2}) + g_T^V \sqrt{Q_+} (M_{B_1} - M_{B_2}) \right. \\
&\quad \left. + f_T^S \sqrt{Q_-} Q_+ - g_T^S \sqrt{Q_+} Q_- \right]. \tag{10}
\end{aligned}$$

where $Q_{\pm} = (M_{B_1} \pm M_{B_2})^2 - q^2$ and $f_i^{(a)}, g_i^{(b)}$, ($i = 1, 2, 3, T$ & $a, b = V, S$) are the various form factors. After integrating out $\cos \theta_l$ in Eqn. (6), one can obtain the q^2 dependent differential decay rate. Besides the branching ratios, other interesting observables in these decay modes are

- Forward-backward asymmetry parameter:

$$A_{FB}(q^2) = \left(\int_{-1}^0 d \cos \theta_l \frac{d^2 \Gamma}{dq^2 d \cos \theta_l} - \int_0^1 d \cos \theta_l \frac{d^2 \Gamma}{dq^2 d \cos \theta_l} \right) / \frac{d\Gamma}{dq^2}. \tag{11}$$

- Convexity parameter:

$$C_F^l(q^2) = \frac{1}{d\Gamma/dq^2} \frac{d^2}{d(\cos \theta_l)^2} \left(\frac{d^2 \Gamma}{dq^2 d \cos \theta_l} \right). \tag{12}$$

- Longitudinal hadron polarization asymmetry parameter:

$$P_L^h(q^2) = \frac{d\Gamma^{\lambda_2=1/2}/dq^2 - d\Gamma^{\lambda_2=-1/2}/dq^2}{d\Gamma/dq^2}, \tag{13}$$

where $d\Gamma^{\lambda_2=\pm 1/2}$ are the individual helicity-dependent differential decay rates, whose detailed expressions are given in Appendix A [33].

- Longitudinal lepton polarization asymmetry parameter:

$$P_L^\tau(q^2) = \frac{d\Gamma^{\lambda_\tau=1/2}/dq^2 - d\Gamma^{\lambda_\tau=-1/2}/dq^2}{d\Gamma/dq^2}, \tag{14}$$

where $d\Gamma^{\lambda_2=\pm 1/2}$ are the individual helicity-dependent differential decay rates, whose detailed expressions are given in Appendix A [33].

- Lepton non-universality parameter:

$$R_{B_2} = \frac{\text{Br}(B_1 \rightarrow B_2 \tau^- \bar{\nu}_\tau)}{\text{Br}(B_1 \rightarrow B_2 l^- \bar{\nu}_l)}, \quad l = e, \mu. \tag{15}$$

- The LHCb Collaboration has measured the ratio of the partially integrated decay rates of $\Lambda_b^0 \rightarrow p \mu \bar{\nu}_l$ over the $\Lambda_b^0 \rightarrow \Lambda_c^+ \mu \bar{\nu}_l$ process as

$$R_{\Lambda_c p}^\mu = \int_{15 \text{ GeV}^2}^{q_{\text{max}}^2} \frac{d\Gamma(\Lambda_b \rightarrow p \mu \bar{\nu}_l)}{dq^2} dq^2 \bigg/ \int_{7 \text{ GeV}^2}^{q_{\text{max}}^2} \frac{d\Gamma(\Lambda_b \rightarrow \Lambda_c \mu \bar{\nu}_l)}{dq^2} dq^2$$

$$= (1.00 \pm 0.04 \pm 0.08) \times 10^{-2} \quad (16)$$

and put constraint on the ratio $|V_{ub}|/|V_{cb}| = 0.083 \pm 0.004 \pm 0.004$ [20]. Similarly, we define the following parameter, to investigate if there is any possible role of NP

$$R_{\Lambda_c p}^\tau = \int_{15 \text{ GeV}^2}^{q_{\text{max}}^2} \frac{d\Gamma(\Lambda_b \rightarrow p \tau \bar{\nu}_\tau)}{dq^2} dq^2 \bigg/ \int_{7 \text{ GeV}^2}^{q_{\text{max}}^2} \frac{d\Gamma(\Lambda_b \rightarrow \Lambda_c \tau \bar{\nu}_\tau)}{dq^2} dq^2. \quad (17)$$

III. CONSTRAINTS ON NEW COUPLINGS

After assembling the expressions for all the interesting observables in presence of NP, we now proceed to constrain the new coefficients by using the experimental bounds on $\text{Br}(B_{u,c} \rightarrow \tau \bar{\nu}_\tau)$, $\text{Br}(B \rightarrow \pi \tau \bar{\nu}_\tau)$, R_π^l , $R_{D^{(*)}}$ and $R_{J/\psi}$ parameters. In this analysis, the new Wilson coefficients are considered as complex. We further assume that only one new coefficient to present at a time and accordingly compute the allowed parameter space of these couplings.

The branching ratios of $B_q \rightarrow l \bar{\nu}_l$ processes in the presence of NP couplings are given by [38]

$$\text{Br}(B_q \rightarrow l \bar{\nu}_l) = \frac{G_F^2 |V_{qb}|^2}{8 \pi} \tau_{B_q} f_{B_q}^2 m_l^2 M_{B_q} \left(1 - \frac{m_l^2}{M_{B_q}^2}\right)^2$$

$$\times \left| (1 + V_L - V_R) - \frac{M_{B_q}^2}{m_l (m_b + m_q)} (S_L - S_R) \right|^2, \quad (18)$$

where M_{B_q} is the mass of B_q meson. By using the masses of all the particles, lifetime of B_q meson, CKM matrix elements from [17] and decay constants $f_{B_u} = 190.5 \pm 4.2$ MeV, $f_{B_c} = 489 \pm 4 \pm 3$ MeV from [39, 40], the branching ratios of $B_{u,c}^+ \rightarrow \tau^+ \nu_\tau$ processes in the SM are found to be

$$\text{Br}(B_u^+ \rightarrow \tau^+ \nu_\tau)|^{\text{SM}} = (8.48 \pm 0.5) \times 10^{-5}, \quad (19)$$

$$\text{Br}(B_c^+ \rightarrow \tau^+ \nu_\tau)|^{\text{SM}} = (3.6 \pm 0.14) \times 10^{-2}. \quad (20)$$

Using the current world average of the B_c lifetime, the upper limit on the branching ratio of $B_c^+ \rightarrow \tau^+ \nu_\tau$ process is [41]

$$\text{Br}(B_c^+ \rightarrow \tau^+ \nu_\tau) \lesssim 30\%. \quad (21)$$

The branching ratios of $B_q \rightarrow Pl\bar{\nu}_l$ ($P = \pi, D$) are given as [42, 43]

$$\begin{aligned} \frac{d\text{Br}(B_q \rightarrow Pl\bar{\nu}_l)}{dq^2} = & \tau_{B_q} \frac{G_F^2 |V_{qb}|^2}{192\pi^3 M_{B_q}^3} q^2 \sqrt{\lambda_P(q^2)} \left(1 - \frac{m_l^2}{q^2}\right)^2 \times \\ & \left\{ |1 + V_L + V_R|^2 \left[\left(1 + \frac{m_l^2}{2q^2}\right) H_0^2 + \frac{3}{2} \frac{m_l^2}{q^2} H_t^2 \right] \right. \\ & + \frac{3}{2} |S_L + S_R|^2 H_S^2 + 8|T_L|^2 \left(1 + \frac{2m_l^2}{q^2}\right) H_T^2 \\ & + 3\text{Re}[(1 + V_L + V_R)(S_L^* + S_R^*)] \frac{m_l}{\sqrt{q^2}} H_S H_t \\ & \left. - 12\text{Re}[(1 + V_L + V_R)T_L^*] \frac{m_l}{\sqrt{q^2}} H_T H_0 \right\}, \end{aligned} \quad (22)$$

where the helicity amplitudes in terms of form factors ($F_{0,+}$) are expressed as

$$\begin{aligned} H_0 &= \sqrt{\frac{\lambda(M_{B_q}^2, m_P^2, q^2)}{q^2}} F_+(q^2), & H_t &= \frac{M_{B_q}^2 - M_P^2}{\sqrt{q^2}} F_0(q^2), \\ H_S &= \frac{M_{B_q}^2 - M_P^2}{m_b - m_q} F_0(q^2) & H_T &= -\frac{\sqrt{\lambda_P(q^2)}}{M_{B_q} + M_P} F_T(q^2). \end{aligned} \quad (23)$$

Using the values of the $B \rightarrow \pi$ form factors from [44–47], the obtained branching ratios of $B_q \rightarrow \pi l \nu_l$ processes, in the SM are given as

$$\text{Br}(B^0 \rightarrow \pi^+ \mu^- \bar{\nu}_\mu)|^{\text{SM}} = (1.35 \pm 0.10) \times 10^{-4}, \quad (24)$$

$$\text{Br}(B^0 \rightarrow \pi^+ \tau^- \bar{\nu}_\tau)|^{\text{SM}} = (9.40 \pm 0.75) \times 10^{-5}. \quad (25)$$

It should be noted that, the branching ratio of the muonic channel agrees reasonably well with the experimental value as given in Eqn. (3), whereas the tau-channel is within its current experimental limit [17]

$$\text{Br}(B^0 \rightarrow \pi^+ \tau^- \bar{\nu}_\tau)|^{\text{Expt}} < 2.5 \times 10^{-4}. \quad (26)$$

The branching ratios of $B_q \rightarrow Vl\bar{\nu}_l$, where $V = D^*, J/\psi$, are given as [42, 43]

$$\begin{aligned}
\frac{d\text{Br}(\bar{B} \rightarrow Vl\bar{\nu}_l)}{dq^2} = & \tau_{B_q} \frac{G_F^2 |V_{qb}|^2}{192\pi^3 M_{B_q}^3} q^2 \sqrt{\lambda_V(q^2)} \left(1 - \frac{m_l^2}{q^2}\right)^2 \times \\
& \left\{ (|1 + V_L|^2 + |V_R|^2) \left[\left(1 + \frac{m_l^2}{2q^2}\right) (H_{V,+}^2 + H_{V,-}^2 + H_{V,0}^2) + \frac{3}{2} \frac{m_l^2}{q^2} H_{V,t}^2 \right] \right. \\
& - 2\text{Re}[(1 + V_L)V_R^*] \left[\left(1 + \frac{m_l^2}{2q^2}\right) (H_{V,0}^2 + 2H_{V,+}H_{V,-}) + \frac{3}{2} \frac{m_l^2}{q^2} H_{V,t}^2 \right] \\
& + \frac{3}{2} |S_L - S_R|^2 H_S^2 + 8|T_L|^2 \left(1 + \frac{2m_l^2}{q^2}\right) (H_{T,+}^2 + H_{T,-}^2 + H_{T,0}^2) \\
& + 3\text{Re}[(1 + V_L - V_R)(S_L^* - S_R^*)] \frac{m_l}{\sqrt{q^2}} H_S H_{V,t} \\
& - 12\text{Re}[(1 + V_L)T_L^*] \frac{m_l}{\sqrt{q^2}} (H_{T,0}H_{V,0} + H_{T,+}H_{V,+} - H_{T,-}H_{V,-}) \\
& \left. + 12\text{Re}[V_R T_L^*] \frac{m_l}{\sqrt{q^2}} (H_{T,0}H_{V,0} + H_{T,+}H_{V,-} - H_{T,-}H_{V,+}) \right\}, \quad (27)
\end{aligned}$$

where $H_{V,\pm}$, $H_{V,0}$, $H_{V,t}$ and H_S are the hadronic amplitudes [42, 43].

In this analysis, we consider the new physics contribution to third generation lepton only and the couplings with light leptons are assumed to be SM like. By allowing only one coefficient at a time, we constrain its real and imaginary parts by comparing the theoretically predicted values of $\text{Br}(B_u^+ \rightarrow \tau^+ \nu_\tau)$ and R_π^l with their corresponding 3σ range of observed experimental results for $b \rightarrow u\tau\bar{\nu}_\tau$ transitions. We have also used the upper limit of the branching ratio of $B^0 \rightarrow \pi^+ \tau^- \bar{\nu}_\tau$ process. In Fig. 1, we show the constraints on real and imaginary parts of new coefficients V_L (top-left panel), V_R (top-right panel), S_L (middle-left panel) and S_R (middle-right panel) obtained from the $\text{Br}(B_u^+ \rightarrow \tau^+ \nu_\tau)$, $\text{Br}(B^0 \rightarrow \pi^+ \tau^- \bar{\nu}_\tau)$ and R_π^l observables. Since the branching ratio of $B_u^+ \rightarrow \tau^+ \nu_\tau$ process does not receive any contribution from tensor operator, the allowed region of real and imaginary parts of tensor coupling (T_L) obtained only from the upper limit on $\text{Br}(B^0 \rightarrow \pi^+ \tau^- \bar{\nu}_\tau)$, and is presented in the bottom panel of this figure. Now imposing the extrema conditions, the allowed range of the new couplings associated with $b \rightarrow u\tau\bar{\nu}_\tau$ transition are presented in Table II. For the case of $b \rightarrow c\tau\bar{\nu}_\tau$ decay processes, the constraints on the real and imaginary parts of individual V_L (top-left panel), V_R (top-right panel), S_L (middle-left panel) and S_R (middle-right panel) coefficients obtained from $R_{D^{(*)}}$ and $R_{J/\psi}$ parameters are shown in Fig. 2. Till now, there is no precise determination of the form factors associated with tensorial operators for $B_c \rightarrow J/\psi l\bar{\nu}_l$ process both from the theoretical and experimental sides. In addition, the leptonic B_c meson decays do not receive any contribution from tensor coupling. Therefore,

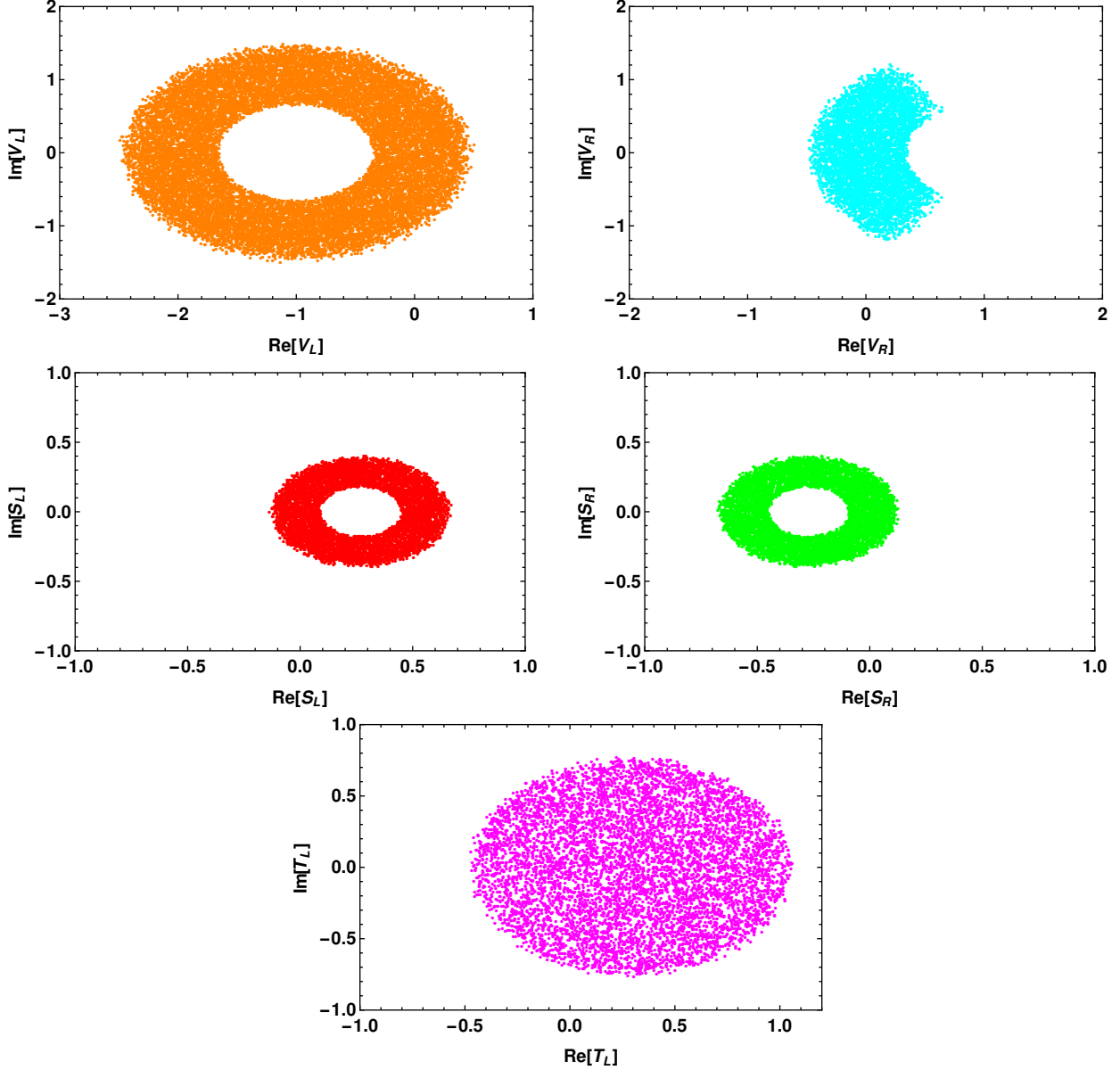


FIG. 1: Constraints on V_L (top-left panel), V_R (top-right panel), S_L (middle-left panel), S_R (middle-right panel) and T_L (bottom panel) coefficients associated with $b \rightarrow u\tau\bar{\nu}_\tau$ transitions, obtained from $\text{Br}(\text{B}_u^+ \rightarrow \tau^+\nu_\tau)$, $\text{Br}(\text{B} \rightarrow \pi\tau\bar{\nu}_\tau)$, R_π^l observables. Here the constraint on T_L coupling is obtained from $\text{Br}(\text{B} \rightarrow \pi\tau\bar{\nu}_\tau)$ experimental data.

the constraints on T_L coupling is obtained from the experimental data on $R_{D^{(*)}}$, which is shown in the bottom panel of Fig. 2. In Table II, we have presented the allowed values of $(\text{Re}[V_{L(R)}] - \text{Im}[V_{L(R)}])$ and $(\text{Re}[S_{L(R)}] - \text{Im}[S_{L(R)}])$ coefficients, which are compatible with the 3σ range of the experimental data.

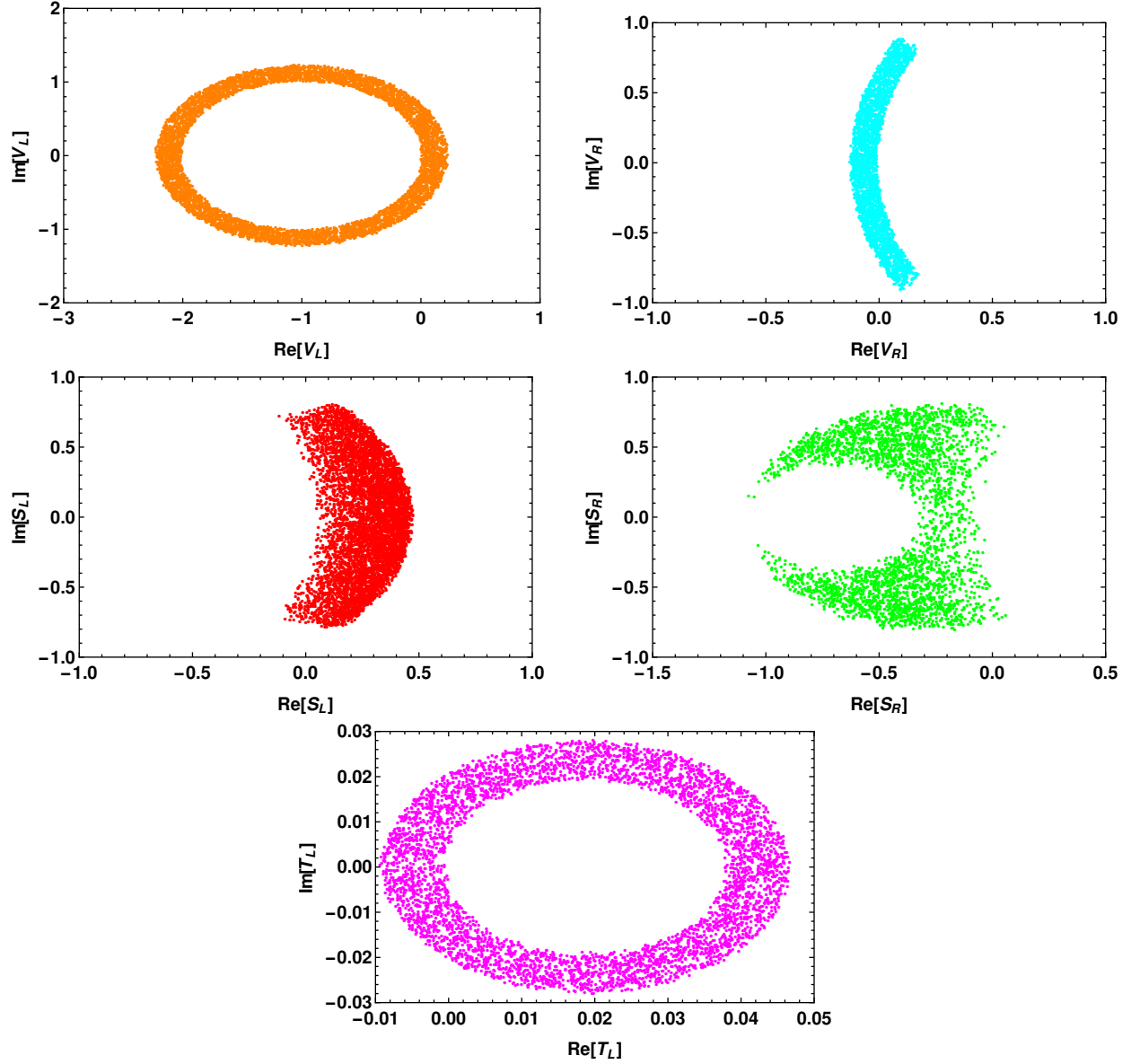


FIG. 2: Constraints on V_L (top-left panel), V_R (top-right panel), S_L (middle-left panel), S_R (middle-right panel) and T_L (bottom panel) new coefficients associated with $b \rightarrow c\tau\bar{\nu}_\tau$ transitions, obtained from $\text{Br}(\text{B}_c^+ \rightarrow \tau^+\nu_\tau)$, $R_{D^{(*)}}$ and $R_{J/\psi}$ observables. Here the constraint on T_L coupling is obtained from $R_{D^{(*)}}$ experimental data.

The constraints on these parameters are obtained earlier from various B decays in Refs. [13, 14, 25, 29, 38, 43, 48–50]. Our analysis is similar to Refs. [25, 32]. In Ref. [25], the authors have considered the couplings to be complex and constrained the new coefficients associated with $b \rightarrow c\tau\bar{\nu}_\tau$ from $R_{D^{(*)}}$ data. However, they have not included the tensor couplings in their analysis, and found that the effects produced by the pseudoscalar coef-

efficient are larger than those obtained from the scalar coefficient. In Ref. [29], the author assumed the couplings as real and computed the allowed parameter space by comparing the $R_{D^{(*)}}$, R_{π}^l parameters with their corresponding 3σ experimental data. In [50], the authors have considered the covariant confined quark model and studied the effect of new physics in the $\bar{B}^0 \rightarrow D^{*}\tau^{-}\bar{\nu}_{\tau}$. They took the new coefficients as complex and constrained them using the experimental values of R_D and $R_{D^{*}}$ within their 2σ range. Recently, the decay process $B_c \rightarrow (J/\psi)\tau\nu_{\tau}$ has been studied, in the covariant confined quark model [49], where the parameter space is constrained by using the experimental values of $R_D, R_{D^{*}}, R_{J/\psi}$ within 2σ range. The new coefficients are considered to be complex and their best fit values are $V_L = -1.05 + i1.15, V_R = 0.04 + i0.60, T_L = 0.38 - i0.06$. Though our analysis is similar to these approaches, but we get more severe bounds on the phases and strengths of the couplings due to additional constraints from $\text{Br}(B_c \rightarrow \tau\nu_{\tau})$ and $R_{J/\psi}$ parameters for $b \rightarrow c\tau\bar{\nu}_{\tau}$ case and from $\text{Br}(B_u \rightarrow \tau\nu_{\tau})$ and $\text{Br}(B \rightarrow \pi\tau\nu_{\tau})$ observables for $b \rightarrow u\tau\bar{\nu}_{\tau}$ process.

TABLE II: Allowed ranges of the new coefficients.

| Decay processes | New coefficients | Minimum value | Maximum Value |
|---------------------------------------|------------------------------------|---------------------|-------------------|
| $b \rightarrow u\tau\bar{\nu}_{\tau}$ | $(\text{Re}[V_L], \text{Im}[V_L])$ | $(-2.489, -1.5)$ | $(0.504, 1.48)$ |
| | $(\text{Re}[V_R], \text{Im}[V_R])$ | $(-0.478, -1.185)$ | $(0.645, 1.198)$ |
| | $(\text{Re}[S_L], \text{Im}[S_L])$ | $(-0.136, -0.396)$ | $(0.672, 0.398)$ |
| | $(\text{Re}[S_R], \text{Im}[S_R])$ | $(-0.6743, -0.398)$ | $(0.1265, 0.398)$ |
| | $(\text{Re}[T_L], \text{Im}[T_L])$ | $(-0.473, -0.773)$ | $(1.07, 0.773)$ |
| $b \rightarrow c\tau\bar{\nu}_{\tau}$ | $(\text{Re}[V_L], \text{Im}[V_L])$ | $(-2.224, -1.228)$ | $(0.225, 1.225)$ |
| | $(\text{Re}[V_R], \text{Im}[V_R])$ | $(-0.129, -0.906)$ | $(0.173, 0.89)$ |
| | $(\text{Re}[S_L], \text{Im}[S_L])$ | $(-0.116, -0.788)$ | $(0.474, 0.8)$ |
| | $(\text{Re}[S_R], \text{Im}[S_R])$ | $(-1.076, -0.809)$ | $(0.06, 0.807)$ |
| | $(\text{Re}[T_L], \text{Im}[T_L])$ | $(-0.0094, -0.028)$ | $(0.0467, 0.028)$ |

IV. NUMERICAL ANALYSIS AND DISCUSSION

In this section, we present the numerical results for semileptonic Λ_b decay modes with third generation leptons in the final state. The masses of all the particles and

the lifetime of Λ_b are taken from [17]. The q^2 dependence of the helicity form factors ($f_{+,\perp,0}$, $g_{+,\perp,0}$, $h_{+,\perp}$, $\tilde{h}_{+,\perp}$) in the lattice QCD calculation can be parametrized as [28, 32]

$$f_i(q^2) = \frac{1}{1 - q^2/(m_{\text{pole}}^f)^2} \left[a_0^f + a_1^f z(q^2) \right], \quad (i = +, \perp, 0) \quad (28)$$

where m_{pole}^f is the pole mass and

$$z(q^2) = \frac{\sqrt{t_+ - q^2} - \sqrt{t_+ - t_0}}{\sqrt{t_+ - q^2} + \sqrt{t_+ - t_0}}, \quad (29)$$

with $t_{\pm} = (M_{B_1} \pm M_{B_2})^2$. The values of the parameters m_{pole}^f , $a_{0,1}^f$ associated with (axial)vector and (pseudo)scalar form factors ($f_{+,\perp,0}$, $g_{+,\perp,0}$) are taken from [28]. In the lattice QCD approach, the m_{pole}^f , $a_{0,1}^f$ parameters linked to tensor form factors ($h_{+,\perp}$, $\tilde{h}_{+,\perp}$) of $\Lambda_b \rightarrow \Lambda_c l \bar{\nu}_l$ process are computed in [32]. However, currently no lattice results are available on the tensor form factors associated with $\Lambda_b \rightarrow pl \bar{\nu}_l$ process. Hence, we relate the tensor form factors of $\Lambda_b \rightarrow pl \bar{\nu}_l$ decay mode with its (axial)vector form factors by using the HQET relations as [33, 51, 52],

$$f_T = g_T = f_1 = \frac{(M_{B_1} + M_{B_2})^2 f_+ - q^2 f_{\perp}}{(M_{B_1} + M_{B_2})^2 - q^2}, \quad f_T^V = g_T^V = f_T^S = g_T^S = 0. \quad (30)$$

The detailed relation between the helicity form factors ($f_{+,\perp,0}$, $g_{+,\perp,0}$, $h_{+,\perp}$, $\tilde{h}_{+,\perp}$) with other various hadronic form factors ($f_{1,2,3}$, $g_{1,2,3}$, f_T , g_T , $f_T^{V(S)}$, $g_T^{V(S)}$) are listed in Appendix B [51]. Using all these input parameters, the predicted branching ratios of $\Lambda_b \rightarrow (\Lambda_c, p) \mu \bar{\nu}_\mu$ processes in the SM are given by

$$\begin{aligned} \text{Br}(\Lambda_b \rightarrow p \mu^- \bar{\nu}_\mu) |^{\text{SM}} &= (4.31 \pm 0.345) \times 10^{-4}, \\ \text{Br}(\Lambda_b \rightarrow \Lambda_c \mu^- \bar{\nu}_\mu) |^{\text{SM}} &= (4.994 \pm 0.4) \times 10^{-2}, \end{aligned} \quad (31)$$

which are in reasonable agreement with the corresponding experimental data [17]

$$\begin{aligned} \text{Br}(\Lambda_b \rightarrow p \mu^- \bar{\nu}_\mu) &= (4.1 \pm 1.0) \times 10^{-4}, \\ \text{Br}(\Lambda_b \rightarrow \Lambda_c l^- \bar{\nu}_l) &= (6.2_{-1.3}^{+1.4}) \times 10^{-2}. \end{aligned} \quad (32)$$

The values of the forward-backward asymmetries in these channels are found to be

$$\langle A_{FB}^\mu \rangle |_{\Lambda_b \rightarrow p}^{\text{SM}} = 0.316 \pm 0.025, \quad \langle A_{FB}^\mu \rangle |_{\Lambda_b \rightarrow \Lambda_c}^{\text{SM}} = 0.19 \pm 0.0152. \quad (33)$$

In Eqn. (31, 33), the theoretical uncertainties are mainly due to the uncertainties associated with the CKM matrix elements and the form factor parameters. After having idea on all

the required input parameters and the allowed parameter space of new couplings, we now proceed to discuss various new physics scenarios and their impact on $\Lambda_b \rightarrow (\Lambda_c, p)\tau\bar{\nu}_\tau$ decay modes in a model independent way.

A. Scenario A: Only V_L coefficient

In this scenario, we assume that the additional new physics contribution to the SM result is coming only from the coupling associated with the left-handed vector like quark currents i.e., $V_L \neq 0$ and $V_R, S_{L,R}, T_L = 0$. Since in this case, the NP operator has the same Lorentz structure as the SM operator, the SM decay rate gets modified by the factor $|1 + V_L|^2$. Imposing 3σ constraint on $\text{Br}(B_{u,c}^+ \rightarrow \tau^+\nu_\tau)$, $\text{Br}(B^0 \rightarrow \pi^+\tau^-\bar{\nu}_\tau)$, R_π^l , $R_{D^{(*)}}$ and $R_{J/\psi}$ observables, the allowed parameter space of V_L couplings associated with $b \rightarrow (u, c)\tau\nu_\tau$ are shown in Figs. 1 and 2 respectively. Using the minimum and maximum values on real

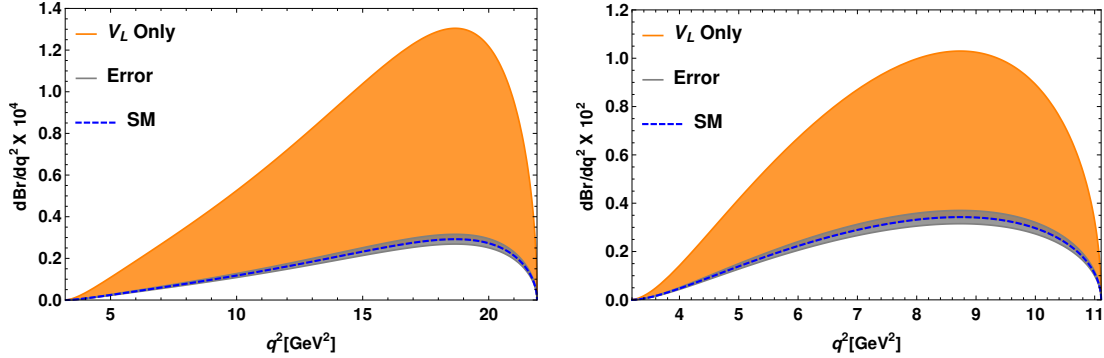


FIG. 3: The q^2 variation of branching ratio of $\Lambda_b \rightarrow p\tau^-\bar{\nu}_\tau$ (left panel) and $\Lambda_b \rightarrow \Lambda_c^+\tau^-\bar{\nu}_\tau$ (right panel) processes in the presence of only V_L new coefficient. Here the orange bands represent the new physics contribution. Blue dashed lines stand for the SM and the theoretical uncertainties arising due to the input parameters are presented in grey color.

and imaginary parts of V_L coefficient from Table II, we present the differential branching ratios of $\Lambda_b \rightarrow p\tau^-\bar{\nu}_\tau$ (left panel) and $\Lambda_b \rightarrow \Lambda_c^+\tau^-\bar{\nu}_\tau$ (right panel) processes with respect to q^2 in Fig. 3. In these figures, the blue dashed lines represent the SM contribution, the orange bands are due to the presence of new V_L coefficient and the grey bands stand for the theoretical uncertainties associated with the input parameters like form factors, CKM matrix elements etc. The branching ratios of $\Lambda_b \rightarrow (\Lambda_c, p)\tau^-\bar{\nu}_\tau$ deviate significantly from their corresponding SM values due to the NP contribution. In addition to the decay rate,

other interesting observables, which can be used to probe new physics, are the zero crossing of the forward-backward asymmetry and the convexity parameters. From Eqn. (12), one can notice that the convexity parameter depends only on the $V_{L,R}$ and T_L couplings. The values for forward-backward asymmetries of $\Lambda_b \rightarrow (\Lambda_c, p)\tau\bar{\nu}_\tau$ processes in the SM are

$$\langle A_{FB}^\tau \rangle|_{\Lambda_b \rightarrow p}^{\text{SM}} = 0.115 \pm 0.0092, \quad \langle A_{FB}^\tau \rangle|_{\Lambda_b \rightarrow \Lambda_c}^{\text{SM}} = -0.09 \pm 0.007, \quad (34)$$

and the corresponding values for the convexity parameters are

$$\langle C_F^\tau \rangle|_{\Lambda_b \rightarrow p}^{\text{SM}} = -0.157 \pm 0.013, \quad \langle C_F^\tau \rangle|_{\Lambda_b \rightarrow \Lambda_c}^{\text{SM}} = -0.098 \pm 0.008. \quad (35)$$

We found no deviation from SM results for the forward-backward asymmetry and convexity parameters due to the presence of V_L coefficient. In Fig. 4, left (right) panel depicts the

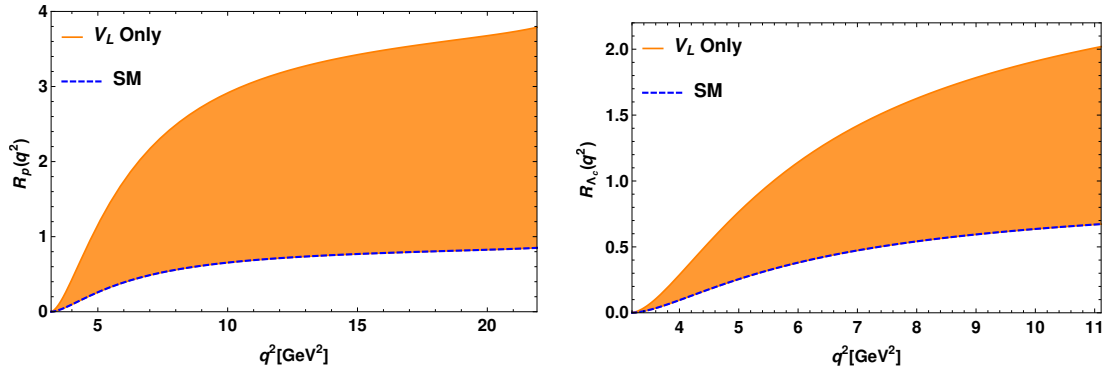


FIG. 4: The variation of R_p (left panel) and R_{Λ_c} (right panel) LNU parameters with respect to q^2 in the presence of only V_L new coefficient.

q^2 variation of lepton universality violating parameters R_p (R_{Λ_c}). We observe that the NP contribution coming from the V_L coupling has significant impact on R_p and R_{Λ_c} parameters. The variation of $R_{\Lambda_c}^\tau$ parameter with q^2 for this case, is presented in the left panel of Fig. 7. The numerical values of the branching ratios and the LNU parameters for both the SM and the V_L -type NP scenario are given in Table III. Besides the branching ratios, forward-backward asymmetry and LNU parameters of $\Lambda_b \rightarrow (\Lambda_c, p)\tau\bar{\nu}_\tau$ processes, the NP effects can also be observed in the hadron and lepton polarization asymmetries. However, no deviation has been found in the presence of V_L coupling from their corresponding SM results.

B. Scenario B: Only V_R coefficient

Here, we assume that only the new V_R coefficient is present in addition to the SM contribution, in the effective Lagrangian (5). To investigate the effect of NP coming from V_R coefficient, we first constrain the new coefficient by imposing 3σ experimental bound on the $b \rightarrow (u, c)\tau\bar{\nu}_\tau$ anomalies. Using the values from Table II, we show the plots for the branching ratios of $\Lambda_b \rightarrow p (\Lambda_c)\tau\bar{\nu}_\tau$ process in the top-left panel (top-right panel) of Fig. 5. In these figures, the cyan bands are due to the additional contribution from V_R coefficient. We notice significant deviation in the branching ratios from their corresponding SM results. The predicted values of the branching ratios for V_R coefficient are presented in Table III. Apart from branching ratios, we are also interested to see the effect of this new coefficient on various q^2 dependent observables. The q^2 variation of the forward backward asymmetry and the convexity parameters for $\Lambda_b \rightarrow p\tau^-\bar{\nu}_\tau$ (left) and $\Lambda_b \rightarrow \Lambda_c\tau^-\bar{\nu}_\tau$ (right) decay processes are depicted in the middle and bottom panels of Fig. 5, respectively. The deviation of convexity parameters from their SM prediction are quite noticeable in these plots. In the presence of V_R coefficient, the numerical values of the C_F^τ parameters are

$$\langle C_F^\tau \rangle|_{\Lambda_b \rightarrow p}^{V_R} = -0.169 \rightarrow -0.147, \quad \langle C_F^\tau \rangle|_{\Lambda_b \rightarrow \Lambda_c}^{V_R} = -0.105 \rightarrow -0.094. \quad (36)$$

The effect of V_R coefficient is found to be rather significant on the forward-backward asymmetry observables of both $\Lambda_b \rightarrow p(\Lambda_c)\tau^-\bar{\nu}_\tau$ decay modes and the corresponding numerical values are

$$\langle A_{FB}^\tau \rangle|_{\Lambda_b \rightarrow p}^{V_R} = -0.248 \rightarrow 0.115, \quad \langle A_{FB}^\tau \rangle|_{\Lambda_b \rightarrow \Lambda_c}^{V_R} = -0.23 \rightarrow -0.09. \quad (37)$$

Left and right panels of Fig. 6, depict the variation of R_p and R_{Λ_c} parameters with respect to q^2 . Though there are no experimental limits on these parameters, significant deviation from their SM values are noticed in the scenario with only V_R coupling. The right panel of Fig. 7 represents the q^2 variation of $R_{\Lambda_c p}^\tau$ parameter. The corresponding numerical values are listed in Table III.

Though the presence of V_L coefficient has no effect on the lepton and hadron polarization asymmetries of $b \rightarrow (u, c)\tau\bar{\nu}_\tau$ decay modes, the V_R coefficient has significant impact on these parameters. In the top panel of Fig. 8, the distribution of the longitudinal polarization components of the daughter baryon p (left panel) and Λ_c (right panel) are shown both

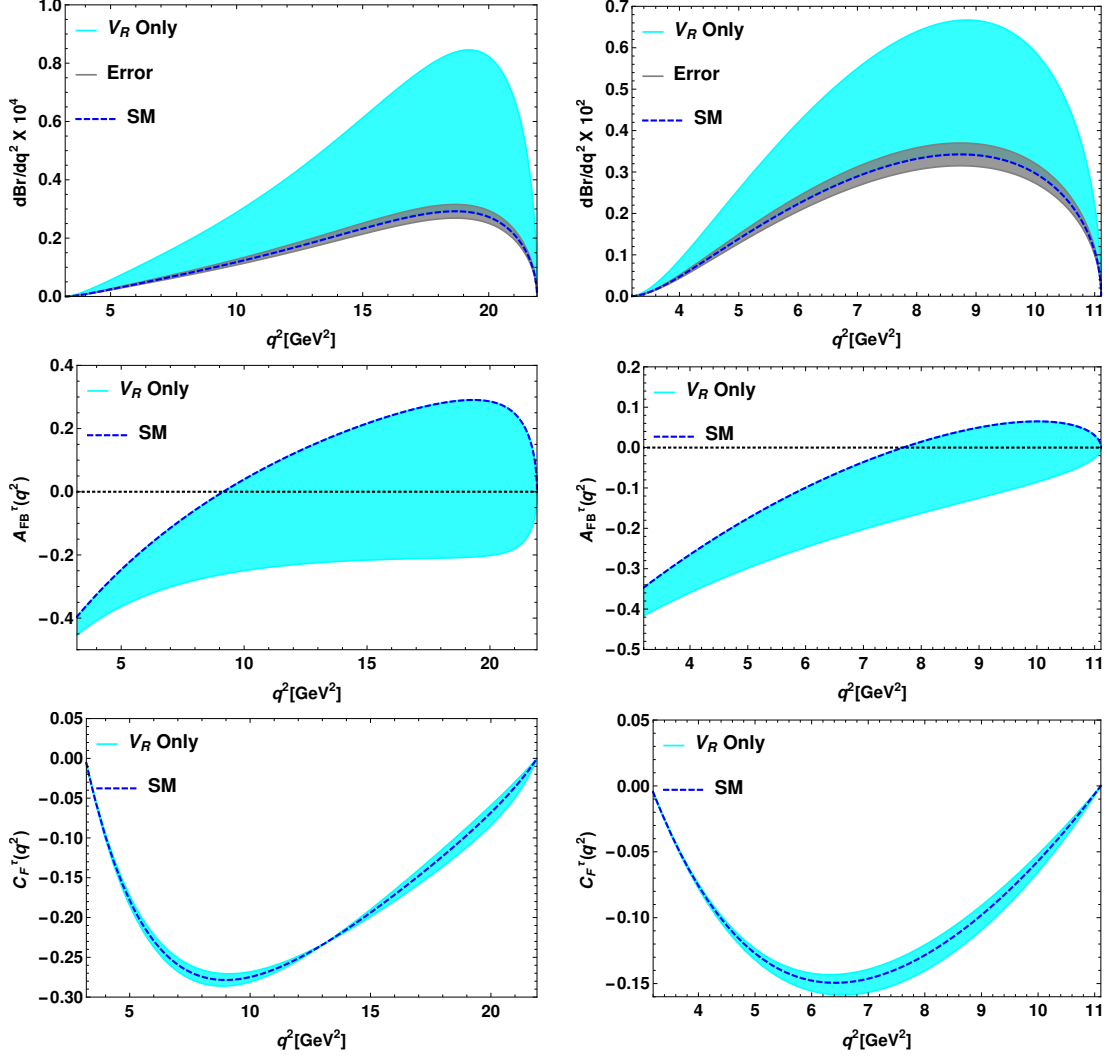


FIG. 5: Top panel represents the q^2 variation of branching ratio of $\Lambda_b \rightarrow p\tau^-\bar{\nu}_\tau$ (left panel) and $\Lambda_b \rightarrow \Lambda_c^+\tau^-\bar{\nu}_\tau$ (right panel) for only V_R new coefficient. The corresponding plots of forward backward asymmetry and the convexity parameters are shown in the middle and bottom panels respectively. Here cyan bands are due to the additional new physics contribution coming from only V_R coefficient.

in the SM and in the presence of only V_R coefficient, and the corresponding plots for the charged τ lepton are presented in the bottom panel. The integrated values of the hadron longitudinal polarization asymmetry parameters in the full physical phase space are

$$\langle P_L^p \rangle_{\Lambda_b \rightarrow p}^{\text{SM}} = -0.897, \quad \langle P_L^{\Lambda_c} \rangle_{\Lambda_b \rightarrow \Lambda_c}^{\text{SM}} = -0.797, \quad (38)$$

$$\langle P_L^p \rangle_{\Lambda_b \rightarrow p}^{V_R \text{ Only}} = -0.897 \rightarrow 0.276, \quad \langle P_L^{\Lambda_c} \rangle_{\Lambda_b \rightarrow \Lambda_c}^{V_R \text{ Only}} = -0.797 \rightarrow -0.068, \quad (39)$$

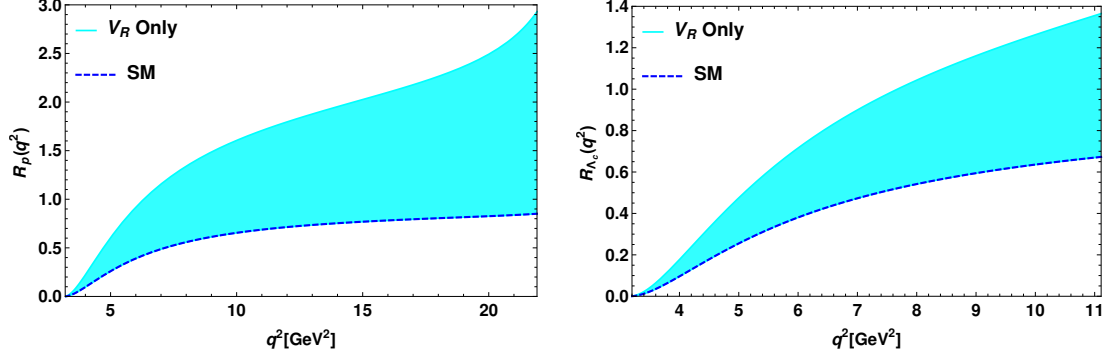


FIG. 6: The variation of R_p (left panel) and R_{Λ_c} (right panel) LNU parameters with respect to q^2 in the presence of only V_R new coefficient.

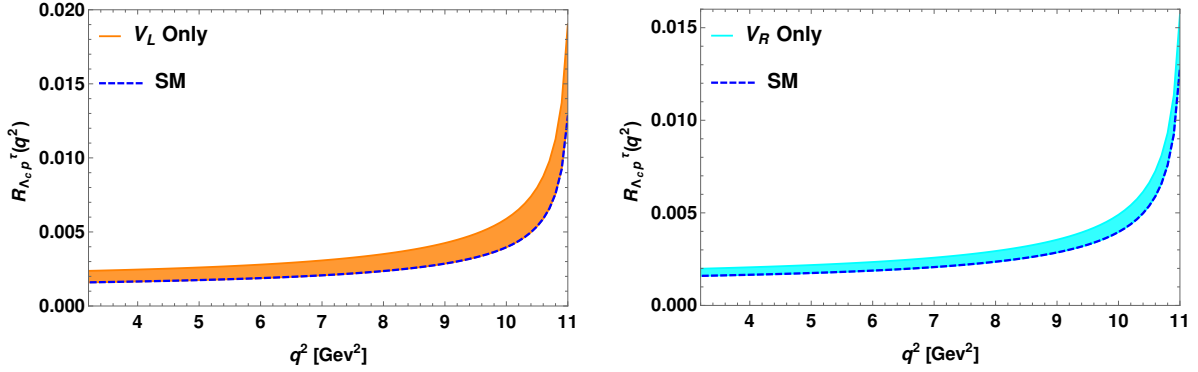


FIG. 7: The variation of $R_{\Lambda_c p}^\tau$ parameter with respect to q^2 in the presence of only V_L (left panel) and V_R (right panel) new coefficients.

and the corresponding numerical values for the charged lepton τ , are

$$\langle P_L^\tau \rangle_{\Lambda_b \rightarrow p}^{\text{SM}} = -0.514, \quad \langle P_L^\tau \rangle_{\Lambda_b \rightarrow \Lambda_c}^{\text{SM}} = -0.207, \quad (40)$$

$$\langle P_L^\tau \rangle_{\Lambda_b \rightarrow p}^{V_R} = -0.577 \rightarrow -0.433, \quad \langle P_L^\tau \rangle_{\Lambda_b \rightarrow \Lambda_c}^{V_R} = -0.25 \rightarrow -0.146. \quad (41)$$

C. Scenario C: Only S_L coefficient

Here, we explore the impact of only S_L coefficient on the angular observables of heavy-heavy and heavy-light semileptonic decays of Λ_b baryon. In section III, we discussed the constraints on the S_L coupling. In the top panel Fig. 9, we present the plots for the differential branching ratios of $\Lambda_b \rightarrow p\tau\bar{\nu}_\tau$ (left) and $\Lambda_b \rightarrow \Lambda_c\tau\bar{\nu}_\tau$ (right) decay processes with respect to q^2 in the presence of S_L coefficient. The corresponding plots for the forward-

TABLE III: The predicted values of branching ratios and lepton non-universality parameters of $\Lambda_b \rightarrow (\Lambda_c, p)\tau\bar{\nu}_\tau$ processes in the SM and in the presence of only $V_{L,R}$ coefficients.

| Observables | SM prediction | Values for V_L coupling | Values for V_R coupling |
|--|-----------------------------------|----------------------------------|--------------------------------|
| $\text{Br}(\Lambda_b \rightarrow p\tau^-\bar{\nu}_\tau)$ | $(2.98 \pm 0.238) \times 10^{-4}$ | $(0.298 - 1.34) \times 10^{-3}$ | $(2.98 - 8.17) \times 10^{-4}$ |
| R_p | 0.692 | $0.692 - 3.09$ | $0.692 - 1.895$ |
| $\text{Br}(\Lambda_b \rightarrow \Lambda_c^+\tau^-\bar{\nu}_\tau)$ | $(1.76 \pm 0.14) \times 10^{-2}$ | $(1.76 - 5.29) \times 10^{-2}$ | $(1.76 - 3.4) \times 10^{-2}$ |
| R_{Λ_c} | 0.353 | $0.353 - 1.06$ | $0.353 - 0.68$ |
| $R_{\Lambda_c p}$ | $(1.693 \pm 0.19) \times 10^{-2}$ | $(1.693 - 2.533) \times 10^{-2}$ | $(1.693 - 2.4) \times 10^{-2}$ |

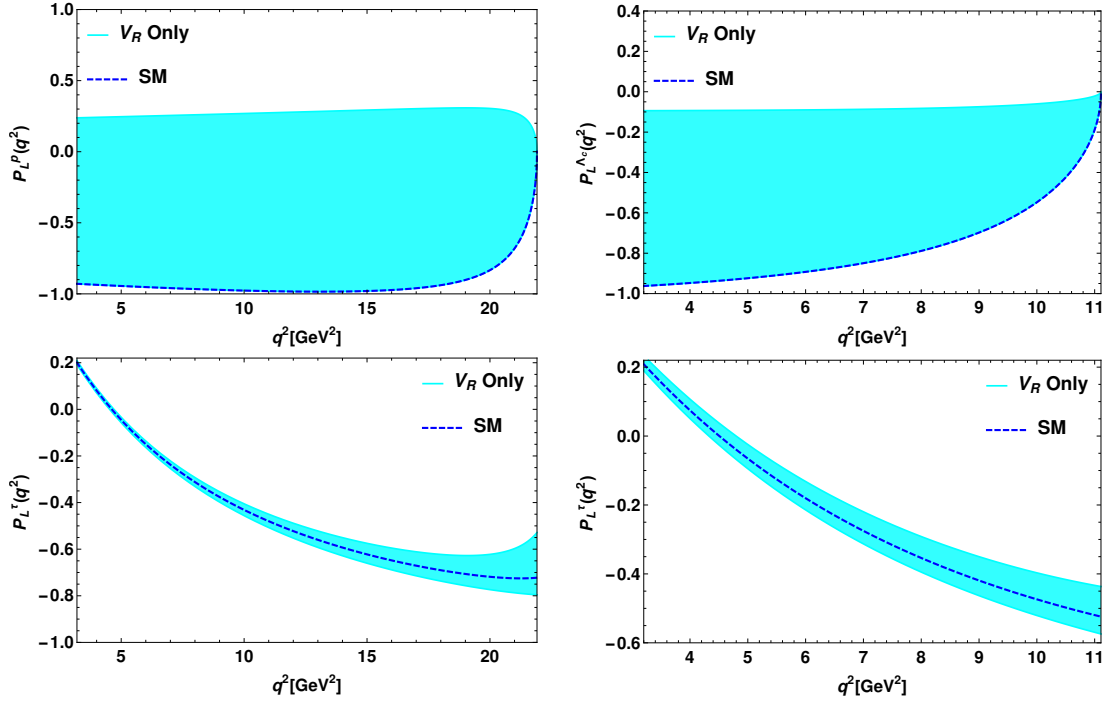


FIG. 8: The plots in the left panel represent the longitudinal polarizations of daughter light baryon p (left-top panel) and the charged τ lepton (left-bottom) with respect to q^2 for only V_R coefficient. The corresponding plots for $\Lambda_b \rightarrow \Lambda_c\tau^-\bar{\nu}_\tau$ mode are shown in the right panel.

backward asymmetry are shown in the bottom panel. In these figures, the red bands stand for the NP contribution from S_L coefficient. The additional contributions provide deviation in the branching ratios and forward-backward asymmetries from their SM values. The q^2 variation of the R_p (left panel) and R_{Λ_c} (right panel) LNU parameters in the presence of S_L coupling are given in Fig. 10. In the presence of only S_L coupling, the longitudinal

polarization components of the p (top-left panel) and Λ_c (top-right panel) daughter baryons with respect to q^2 are presented in the top panel of Fig. 11 and the bottom panel depicts the longitudinal lepton polarization asymmetry parameters for $\Lambda_b \rightarrow p(\Lambda_c)\tau\bar{\nu}_\tau$ processes. The lepton polarization asymmetry parameters provide profound deviation from the SM in comparison to their longitudinal hadron polarization parameters. The top-left panel of Fig. 18 shows the variation of $R_{\Lambda_c p}^\tau$ parameter with q^2 . In Table IV, we report the numerical values of all these parameters.

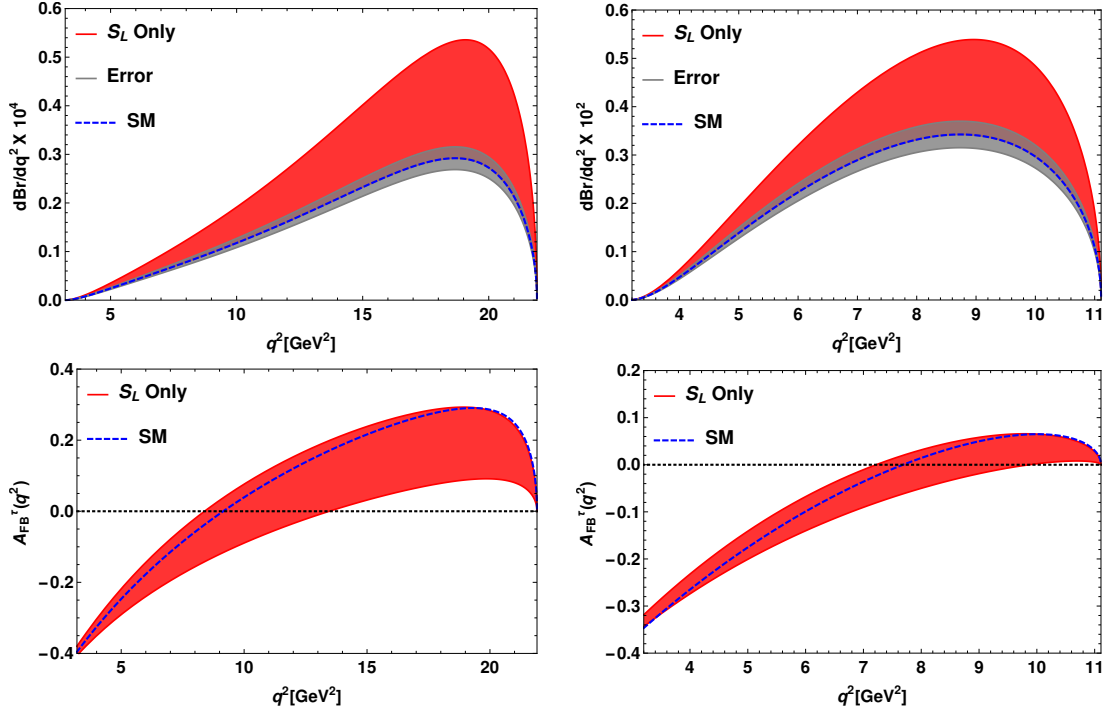


FIG. 9: Top panel represents the q^2 variation of branching ratios of $\Lambda_b \rightarrow p\tau^-\bar{\nu}_\tau$ (left panel) and $\Lambda_b \rightarrow \Lambda_c^+\tau^-\bar{\nu}_\tau$ (right panel) decay modes in the presence of only S_L new coefficient. The corresponding plots for forward-backward asymmetries are shown in the bottom panel. Here red bands are due to the additional new physics contribution coming from only S_L coefficient.

D. Scenario D: Only S_R coefficient

In this subsection, we perform an analysis for semileptonic decay modes of Λ_b baryon with the additional S_R coupling. Using the allowed ranges of the real and imaginary part of S_R coupling from Table II, the branching ratios of $\Lambda_b \rightarrow p\tau\bar{\nu}_\tau$ (left) and $\Lambda_b \rightarrow \Lambda_c\tau\bar{\nu}_\tau$

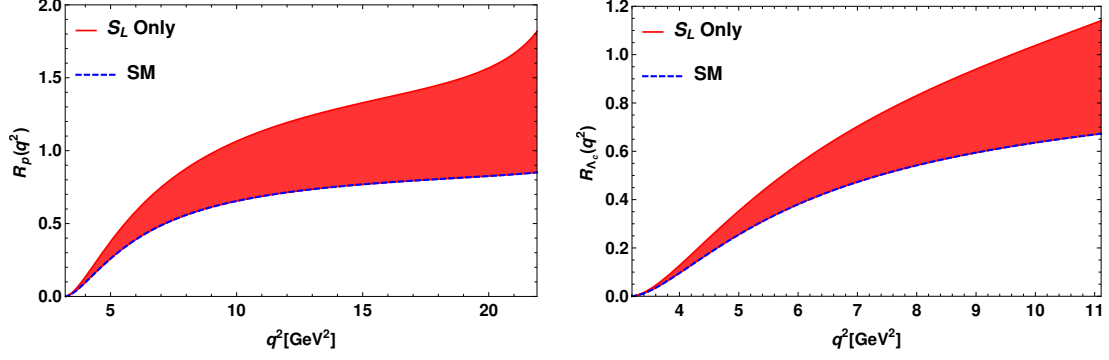


FIG. 10: The variation of R_p (left panel) and R_{Λ_c} (right panel) with respect to q^2 in the presence of only S_L coefficient.

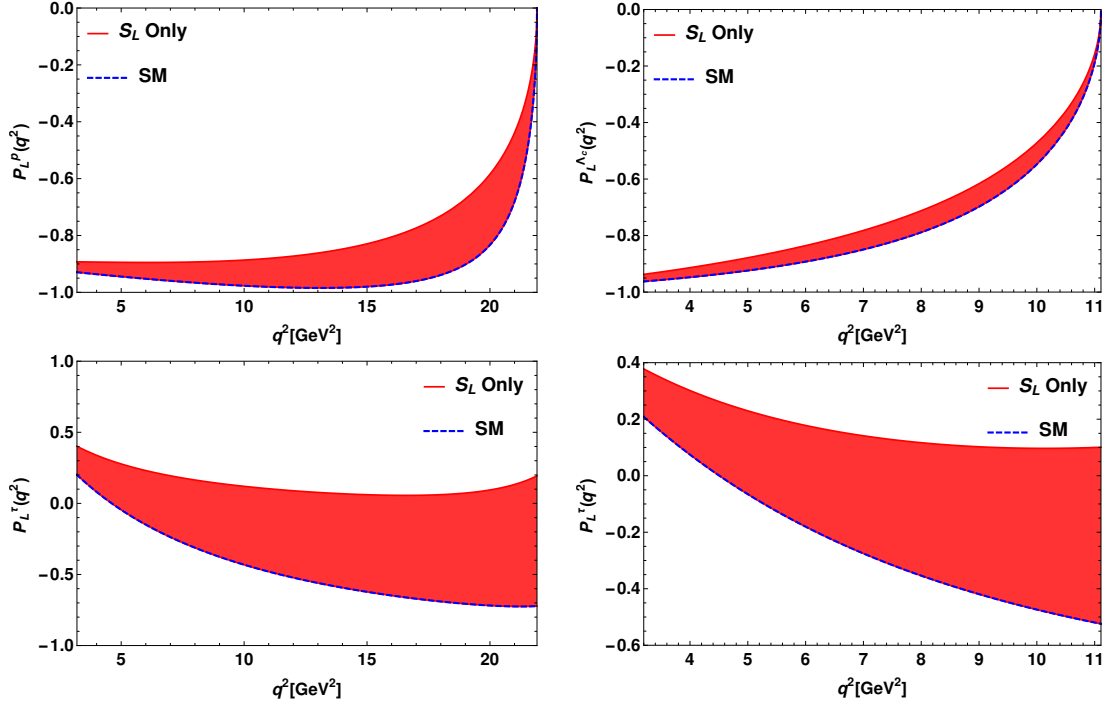


FIG. 11: The plots in the left panel represent the longitudinal polarizations of daughter light baryon p (left-top panel) and the charged τ lepton (left-bottom) with respect to q^2 for only S_L coefficient. The corresponding plots for $\Lambda_b \rightarrow \Lambda_c \tau^- \bar{\nu}_\tau$ mode are shown in the right panel.

(right) decay processes with respect to q^2 are presented in Fig. 12. The bottom panel of this figure represents the q^2 variation of the forward-backward asymmetry for $\Lambda_b \rightarrow p \tau^- \bar{\nu}_\tau$ (left) and $\Lambda_b \rightarrow \Lambda_c \tau^- \bar{\nu}_\tau$ (right). In these figures, the green bands are due to the additional new contribution of S_R coefficient to the SM. We observe profound deviation in the branching ratios and forward-backward asymmetries of these decay modes from their SM values. Left

(right) panel of Fig. 13, show the effect of S_R coupling on the q^2 variation of R_p (R_{Λ_c}) parameter. The longitudinal polarization components of the p (top-left panel) and Λ_c (top-right panel) daughter baryons with respect to q^2 in the presence of contribution from only S_R coefficient, are presented in the top panel of Fig. 14 and the bottom panel depict the longitudinal lepton polarization asymmetry parameters for $\Lambda_b \rightarrow p(\Lambda_c)\tau\bar{\nu}_\tau$ processes. We notice significant deviation of hadron and lepton polarization asymmetries from their corresponding SM values due to additional contribution from S_R coupling. The plot for the $R_{\Lambda_{cp}}^\tau$ parameter with q^2 in the presence of only S_R coefficient is presented in the right panel of Fig. 18. The numerical values of all these parameters are presented in Table IV. Since the convexity parameters are independent of scalar type couplings, the $S_{L,R}$ coefficients play no role for this parameter.

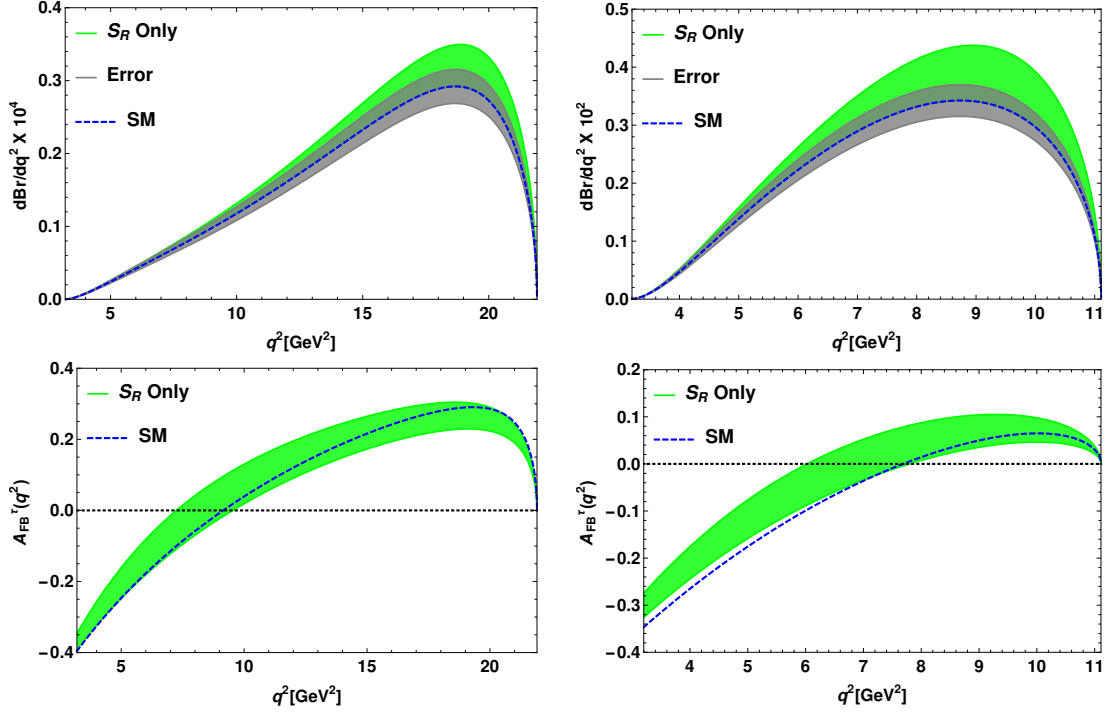


FIG. 12: Top panel represents the q^2 variation of branching ratios of $\Lambda_b \rightarrow p\tau^-\bar{\nu}_\tau$ (left panel) and $\Lambda_b \rightarrow \Lambda_c^+\tau^-\bar{\nu}_\tau$ (right panel) decay processes in the presence of only S_R coefficient. The corresponding plots for the forward-backward asymmetries are shown in the bottom panel. Here green bands stand for the additional new physics contribution coming from only S_R coefficient.

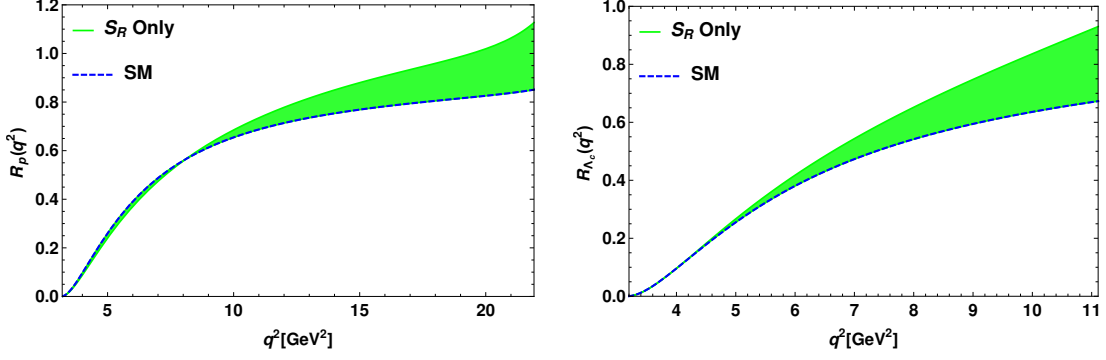


FIG. 13: The variation of R_p (left panel) and R_{Λ_c} (right panel) with respect to q^2 in the presence of only S_R coefficient.

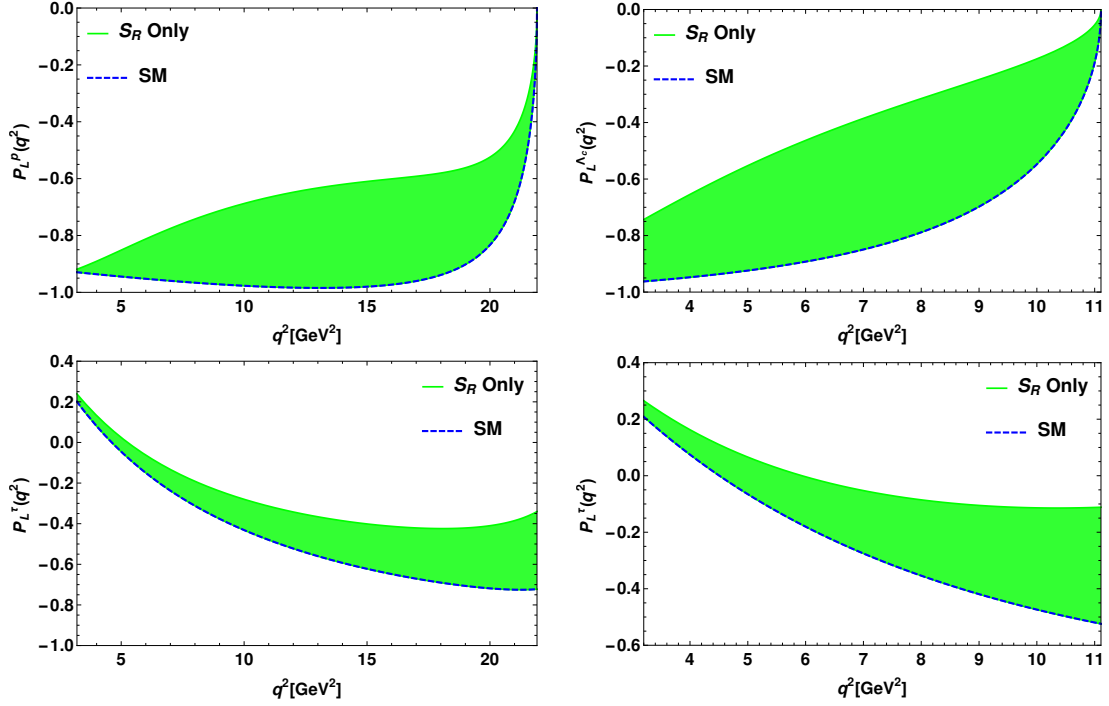


FIG. 14: The plots in the left panel represent the longitudinal polarizations of daughter light baryon p (left-top panel) and the charged τ lepton (left-bottom) with respect to q^2 for only S_R coefficient. The corresponding plots for $\Lambda_b \rightarrow \Lambda_c \tau^- \bar{\nu}_\tau$ mode are shown in the right panel.

E. Scenario E: Only T_L coefficient

The sensitivity of tensor coupling on various physical observables associated with semileptonic baryonic $b \rightarrow (c, u) \tau^- \bar{\nu}_\tau$ decay processes will be investigated in this subsection. The allowed region of real and imaginary parts of the tensor coupling are presented in section

III. Using all the input parameters and the constrained new tensor coefficient, we show the q^2 variation of branching ratio (left-top panel), forward-backward asymmetry (left-middle panel) and convexity parameter (left-bottom panel) of $\Lambda_b \rightarrow p\tau\bar{\nu}_\tau$ decay mode in the left panel of Fig. 15. The right panel of this figure represents the corresponding plots for $\Lambda_b \rightarrow \Lambda_c\tau\bar{\nu}_\tau$ process. Here the magenta bands represent the additional contribution coming from the new T_L coefficient. For $\Lambda_b \rightarrow p\tau\bar{\nu}_\tau$ process, as the bound on T_L is weak, the branching ratio, forward-backward asymmetry and the convexity parameter deviate significantly from their SM predictions compared to the observables for $\Lambda_b \rightarrow \Lambda_c\tau\bar{\nu}_\tau$ process. For $\Lambda_b \rightarrow \Lambda_c\tau\bar{\nu}_\tau$ process, the deviations are quite minimal as the coefficient T_L is severely constrained. In the presence of T_L coefficient, the numerical values of the convexity parameters are

$$\langle C_F^\tau \rangle|_{\Lambda_b \rightarrow p}^{T_L} = -0.017 \rightarrow -0.027, \quad \langle C_F^\tau \rangle|_{\Lambda_b \rightarrow \Lambda_c}^{T_L} = -0.121 \rightarrow -0.098. \quad (42)$$

The plots for the lepton nonuniversality parameter R_p (left panel) and R_{Λ_c} (right panel) are shown in Fig. 16. The top panel of Fig. 17 represents the hadron polarization asymmetry parameters of $\Lambda_b \rightarrow p\tau\bar{\nu}_\tau$ (left panel) and $\Lambda_b \rightarrow \Lambda_c\tau\bar{\nu}_\tau$ (right panel) process and the corresponding plots for lepton polarization asymmetries are given in the bottom panel of this figure. We observe that, the LNU parameter, longitudinal hadron and lepton polarization asymmetries of $\Lambda_b \rightarrow p\tau\bar{\nu}_\tau$ process have large deviation from their SM values due to the presence of tensor coupling, whereas negligible deviations (R_{Λ_c} has some deviation from its SM result) are noticed for the observables of $\Lambda_b \rightarrow \Lambda_c\tau\bar{\nu}_\tau$ decay mode. The q^2 variation of $R_{\Lambda_{cp}}^\tau$ parameter is depicted in the bottom panel of Fig. 18. Table IV shows the integrated values of all these angular observables.

V. CONCLUSION

In this work, we have performed a model independent analysis of baryonic $\Lambda_b \rightarrow (\Lambda_c, p)l\bar{\nu}_l$ decay processes by considering the generalized effective Lagrangian in the presence of new physics. We considered the new couplings to be complex in our analysis. In order to constrain the new couplings, we have assumed that only one coefficient to be present at a time and constrained the new coefficients by comparing the theoretical predictions of $\text{Br}(B_{u,c}^+ \rightarrow \tau^+\nu_\tau)$, $\text{Br}(B \rightarrow \pi\tau\bar{\nu}_\tau)$, R_π^l , $R_{D^{(*)}}$ and $R_{J/\psi}$ observables with their measured experimental data.

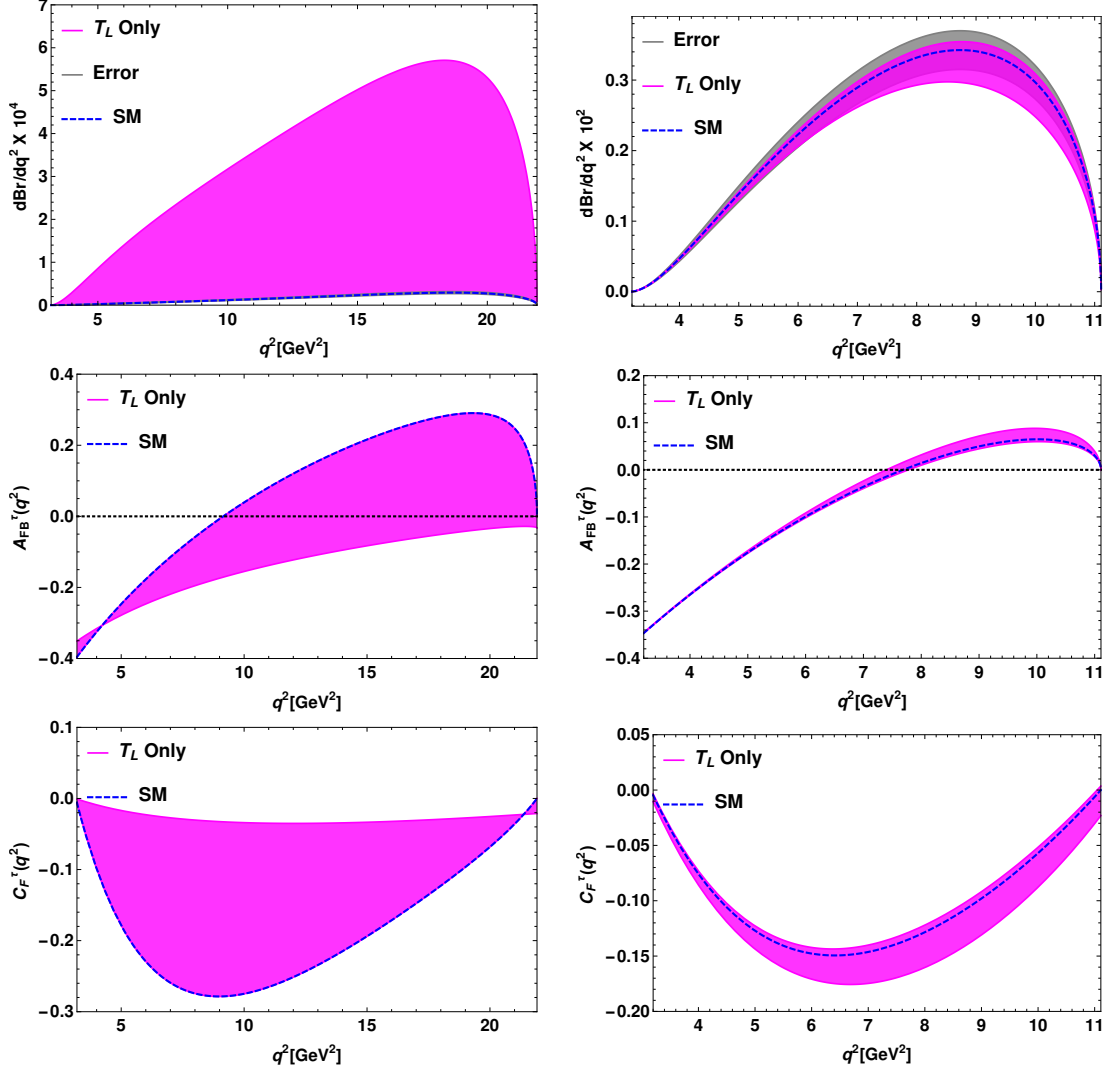


FIG. 15: Top panel represents the q^2 variation of branching ratio of $\Lambda_b \rightarrow p\tau^-\bar{\nu}_\tau$ (left panel) and $\Lambda_b \rightarrow \Lambda_c^+\tau^-\bar{\nu}_\tau$ (right panel) for only T_L new coefficient. The corresponding plots of forward backward asymmetry and the convexity parameters are shown in the middle and bottom panels respectively. Here magenta bands are due to the additional new physics contribution coming from only T_L coefficient.

Using the allowed parameter space, we estimated the branching ratios, forward-backward asymmetries, convexity parameters of $\Lambda_b \rightarrow (\Lambda_c, p)l\bar{\nu}_\tau$ decay processes. We also investigated the longitudinal polarization components of the daughter baryon (p, Λ_c) and the final state charged lepton, τ . The convexity parameter only depend on the (axial)vector and tensor type couplings and are independent of the $S_{L,R}, T_L$ coefficients. Inspired by the observation of lepton non-universality parameters in various B meson decays, we have also scrutinized

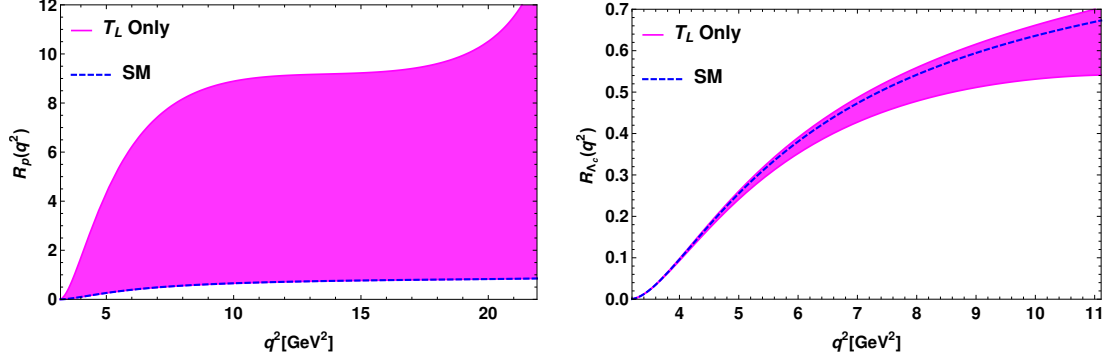


FIG. 16: The variation of R_p (left panel) and R_{Λ_c} (right panel) with respect to q^2 in the presence of only T_L coefficient.

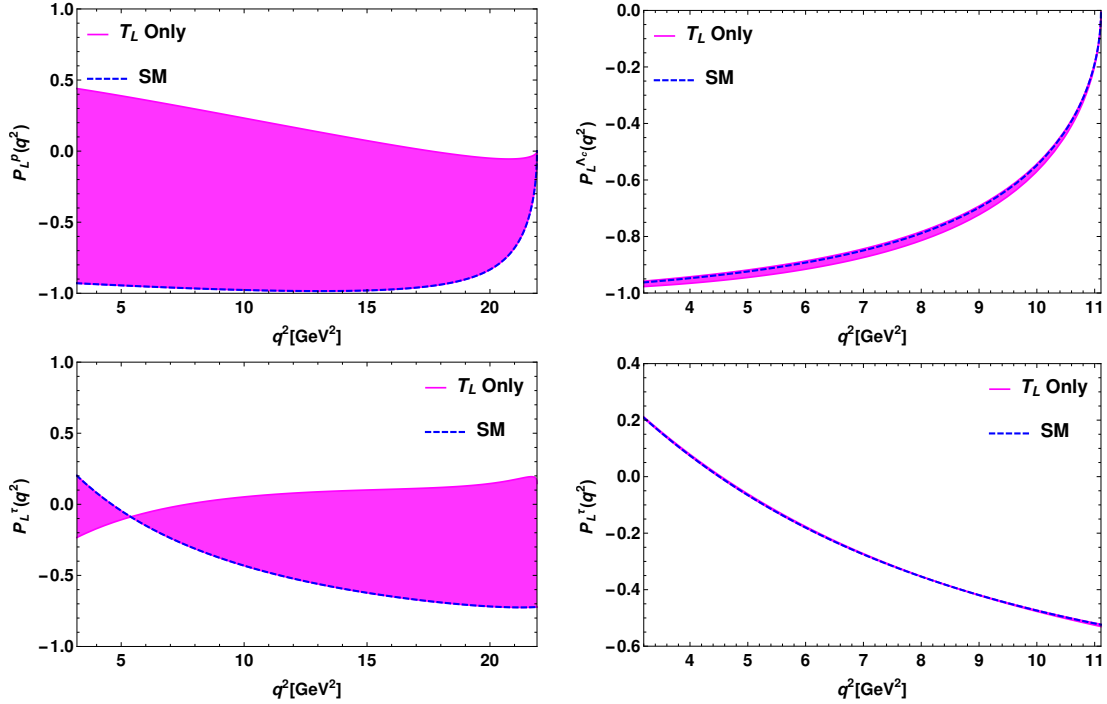


FIG. 17: The plots in the left panel represent the longitudinal polarizations of daughter light baryon p (left-top panel) and the charged τ lepton (left-bottom) with respect to q^2 for only T_L coefficient. The corresponding plots for $\Lambda_b \rightarrow \Lambda_c \tau^- \bar{\nu}_\tau$ mode are shown in the right panel.

the lepton universality violating parameters ($R_p, R_{\Lambda_c}, R_{\Lambda_{cp}}^\tau$) in the baryonic decay modes. We found significant deviation in the branching ratios and the R_p , R_{Λ_c} , $R_{\Lambda_{cp}}$ parameters from their corresponding standard model values, in the presence of additional new vector like coupling (V_L coefficient). However, such coupling does not affect the convexity pa-

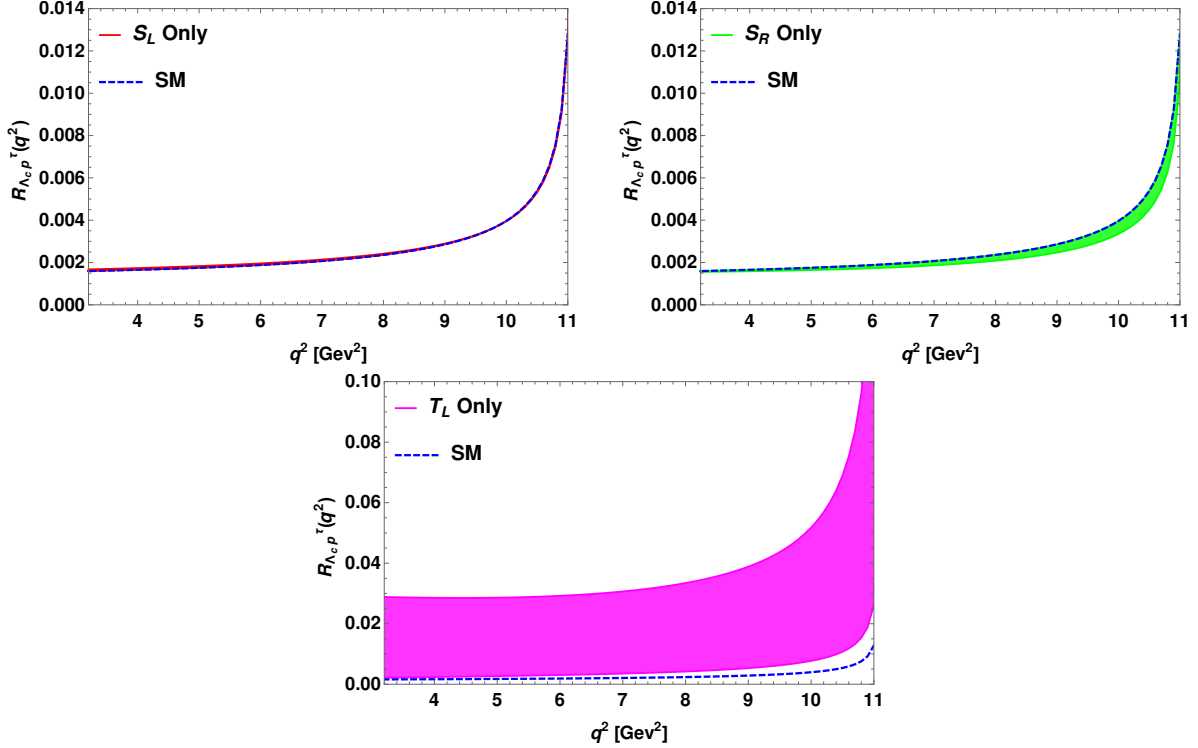


FIG. 18: The variation of $R_{\Lambda_c p}^\tau$ parameter with respect to q^2 in the presence of only S_L (top-left panel), S_R (top-right panel) and T_L (bottom panel) coefficients.

parameter, forward-backward asymmetries, lepton and hadron polarization asymmetries. We further, noticed profound deviation in the branching ratios and all other angular observables of semileptonic baryonic $b \rightarrow (u, c)\tau\bar{\nu}_l$ decay processes due to the additional contribution of V_R coupling to the SM. The branching ratios, forward-backward asymmetries, longitudinal hadron and lepton polarization asymmetry parameter and the LNU observables deviate significantly from their corresponding standard model results in the presence of $S_{L,R}$ coefficients. These coefficients do not have significant effect on $R_{\Lambda_c p}$ parameter. We have also computed the branching ratio, forward-backward asymmetry, convexity parameter, hadron and lepton polarization asymmetries and LNU parameter of $\Lambda_b \rightarrow p(\Lambda_c)\tau\bar{\nu}_\tau$ decay process by using the additional contribution from new tensor (T_L) coupling. All the angular observables of $\Lambda_b \rightarrow p\tau\bar{\nu}_\tau$ process receive significant deviations from their SM values, compared to the corresponding parameters of $\Lambda_b \rightarrow \Lambda_c\tau\bar{\nu}_\tau$ decay mode. To conclude, we have explored the effect of individual complex $V_{L,R}$, $S_{L,R}$ and T_L couplings on the angular observables of baryonic decays of Λ_b baryon. We found profound deviation from the standard model results due to the presence of these new couplings. We noticed that the V_R and S_L couplings

TABLE IV: The predicted values of branching ratios, forward-backward asymmetries, longitudinal hadron ad lepton polarization asymmetries and lepton non-universality parameters of $\Lambda_b \rightarrow (\Lambda_c, p)\tau\bar{\nu}_\tau$ processes in the SM and in the presence of only $S_{L,R}$ and T_L new coefficients.

| Observables | Values for S_L coupling | Values for S_R coupling | Values for T_L coupling |
|--|---------------------------------|----------------------------------|---------------------------------|
| $\text{Br}(\Lambda_b \rightarrow p\tau^-\bar{\nu}_\tau)$ | $(2.98 - 5.25) \times 10^{-4}$ | $(2.98 - 3.48) \times 10^{-4}$ | $(0.298 - 6.68) \times 10^{-3}$ |
| A_{FB}^τ | $-0.019 \rightarrow 0.139$ | $0.086 \rightarrow 0.177$ | $-0.172 \rightarrow -0.125$ |
| P_L^p | $-0.896 \rightarrow -0.73$ | $-0.896 \rightarrow -0.6$ | $-0.896 \rightarrow 0.337$ |
| P_L^τ | $-0.515 \rightarrow 0.123$ | $-0.515 \rightarrow -0.31$ | $-0.515 \rightarrow 0.037$ |
| R_p | $0.692 - 1.266$ | $0.692 - 0.81$ | $0.692 - 8.8$ |
| $\text{Br}(\Lambda_b \rightarrow \Lambda_c^+\tau^-\bar{\nu}_\tau)$ | $(1.76 - 2.7) \times 10^{-2}$ | $(1.76 - 2.2) \times 10^{-2}$ | $(1.553 - 1.82) \times 10^{-2}$ |
| A_{FB}^τ | $-0.121 \rightarrow -0.06$ | $-0.786 \rightarrow -0.005$ | $-0.034 \rightarrow -0.09$ |
| $P_L^{\Lambda_c}$ | $-0.796 \rightarrow -0.725$ | $-0.796 \rightarrow -0.4$ | $-0.79 \rightarrow -0.812$ |
| P_L^τ | $-0.207 \rightarrow 0.178$ | $-0.207 \rightarrow -0.0021$ | -0.207 |
| R_{Λ_c} | $0.353 - 0.539$ | $0.353 - 0.44$ | $0.31 \rightarrow 0.364$ |
| R_{Λ_cp} | $(1.693 - 1.95) \times 10^{-2}$ | $(1.582 - 1.693) \times 10^{-2}$ | $0.0192 - 0.367$ |

significantly affect all the observables and the tensor coupling plays a vital role in the case of $\Lambda_b \rightarrow p\tau\bar{\nu}_\tau$ decay mode. Though there is no experimental measurement on these baryonic $b \rightarrow (u, c)\tau\bar{\nu}_\tau$ decay processes, the study of these modes are found to be very crucial in order to shed light on the nature of new physics.

Acknowledgments

RM would like to thank Science and Engineering Research Board (SERB), Government of India for financial support through grant No. SB/S2/HEP-017/2013. AR acknowledges University Grants Commission for financial support.

Appendix A: Helicity-dependent differential decay rates

The expressions for the helicity-dependent differential decay rates required to analyze the longitudinal hadron and lepton polarization asymmetries are given by [33]

$$\begin{aligned}
\frac{d\Gamma^{\lambda_2=1/2}}{dq^2} &= \frac{m_l^2}{q^2} \left[\frac{4}{3} (H_{\frac{1}{2},+}^2 + H_{\frac{1}{2},0}^2 + 3H_{\frac{1}{2},t}^2) + \frac{2}{3} (H_{\frac{1}{2},+,-}^{T^2} + H_{\frac{1}{2},0,t}^{T^2} + H_{\frac{1}{2},+,0}^{T^2} + H_{\frac{1}{2},+,t}^{T^2} \right. \\
&\quad \left. + 2H_{\frac{1}{2},+,-}^T H_{\frac{1}{2},0,t}^T + 2H_{\frac{1}{2},+,0}^T H_{\frac{1}{2},+,t}^T) \right] + \frac{8}{3} (H_{\frac{1}{2},0}^2 + H_{\frac{1}{2},+}^2) + 4H_{\frac{1}{2},0}^{SP^2} \\
&\quad + \frac{1}{3} (H_{\frac{1}{2},+,-}^{T^2} + H_{\frac{1}{2},0,t}^{T^2} + H_{\frac{1}{2},+,0}^{T^2} + H_{\frac{1}{2},+,t}^{T^2} + 2H_{\frac{1}{2},+,-}^T H_{\frac{1}{2},0,t}^T + 2H_{\frac{1}{2},+,0}^T H_{\frac{1}{2},+,t}^T) \\
&\quad + \frac{4m_l}{\sqrt{q^2}} \left[(H_{\frac{1}{2},0} H_{\frac{1}{2},+,-}^T + H_{\frac{1}{2},0} H_{\frac{1}{2},0,t}^T + H_{\frac{1}{2},+} H_{\frac{1}{2},+,0}^T + H_{\frac{1}{2},+} H_{\frac{1}{2},+,t}^T) \right. \\
&\quad \left. + 2(H_{\frac{1}{2},t} H_{\frac{1}{2},0}^{SP}) \right], \\
\frac{d\Gamma^{\lambda_2=-1/2}}{dq^2} &= \frac{m_l^2}{q^2} \left[\frac{4}{3} (H_{-\frac{1}{2},-}^2 + H_{-\frac{1}{2},0}^2 + 3H_{-\frac{1}{2},t}^2) + \frac{2}{3} (H_{-\frac{1}{2},+,-}^{T^2} + H_{-\frac{1}{2},0,t}^{T^2} + H_{-\frac{1}{2},0,-}^{T^2} + H_{-\frac{1}{2},-,t}^{T^2} \right. \\
&\quad \left. + 2H_{-\frac{1}{2},+,-}^T H_{-\frac{1}{2},0,t}^T + 2H_{-\frac{1}{2},0,-}^T H_{-\frac{1}{2},-,t}^T) \right] + \frac{8}{3} (H_{-\frac{1}{2},-}^2 + H_{-\frac{1}{2},0}^2) + 4H_{-\frac{1}{2},0}^{SP^2} \\
&\quad + \frac{1}{3} (H_{-\frac{1}{2},+,-}^{T^2} + H_{-\frac{1}{2},0,t}^{T^2} + H_{-\frac{1}{2},0,-}^{T^2} + H_{-\frac{1}{2},-,t}^{T^2} + 2H_{-\frac{1}{2},+,-}^T H_{-\frac{1}{2},0,t}^T + 2H_{-\frac{1}{2},0,-}^T H_{-\frac{1}{2},-,t}^T) \\
&\quad + \frac{4m_l}{\sqrt{q^2}} \left[(H_{-\frac{1}{2},0} H_{-\frac{1}{2},+,-}^T + H_{-\frac{1}{2},0} H_{-\frac{1}{2},0,t}^T + H_{-\frac{1}{2},-} H_{-\frac{1}{2},0,-}^T + H_{-\frac{1}{2},-} H_{-\frac{1}{2},-,t}^T) \right. \\
&\quad \left. + 2(H_{-\frac{1}{2},t} H_{-\frac{1}{2},0}^{SP}) \right], \\
\frac{d\Gamma^{\lambda_\tau=1/2}}{dq^2} &= \frac{m_l^2}{q^2} \left[\frac{4}{3} (H_{\frac{1}{2},+}^2 + H_{\frac{1}{2},0}^2 + H_{-\frac{1}{2},-}^2 + H_{-\frac{1}{2},0}^2) + 4(H_{\frac{1}{2},t}^2 + H_{-\frac{1}{2},t}^2) \right] + 4(H_{\frac{1}{2},0}^{SP^2} + H_{-\frac{1}{2},0}^{SP^2}) \\
&\quad + \frac{1}{3} \left[H_{\frac{1}{2},+,-}^{T^2} + H_{\frac{1}{2},0,t}^{T^2} + H_{\frac{1}{2},+,0}^{T^2} + H_{\frac{1}{2},+,t}^{T^2} + H_{-\frac{1}{2},+,-}^{T^2} + H_{-\frac{1}{2},0,t}^{T^2} + H_{-\frac{1}{2},0,-}^{T^2} + H_{-\frac{1}{2},-,t}^{T^2} \right. \\
&\quad \left. + 2(H_{\frac{1}{2},+,-}^T H_{\frac{1}{2},0,t}^T + H_{\frac{1}{2},+,0}^T H_{\frac{1}{2},+,t}^T + H_{-\frac{1}{2},+,-}^T H_{-\frac{1}{2},0,t}^T + H_{-\frac{1}{2},0,-}^T H_{-\frac{1}{2},-,t}^T) \right] \\
&\quad + \frac{4m_l}{3\sqrt{q^2}} \left[6(H_{\frac{1}{2},t} H_{\frac{1}{2},0}^{SP} + H_{-\frac{1}{2},t} H_{-\frac{1}{2},0}^{SP}) + (H_{\frac{1}{2},0} H_{\frac{1}{2},+,-}^T + H_{\frac{1}{2},0} H_{\frac{1}{2},0,t}^T \right. \\
&\quad \left. + H_{\frac{1}{2},+} H_{\frac{1}{2},+,0}^T + H_{\frac{1}{2},+} H_{\frac{1}{2},+,t}^T + H_{-\frac{1}{2},0} H_{-\frac{1}{2},+,-}^T + H_{-\frac{1}{2},0} H_{-\frac{1}{2},0,t}^T + H_{-\frac{1}{2},-} H_{-\frac{1}{2},0,-}^T \right. \\
&\quad \left. + H_{-\frac{1}{2},-} H_{-\frac{1}{2},-,t}^T) \right], \\
\frac{d\Gamma^{\lambda_\tau=-1/2}}{dq^2} &= \frac{8}{3} (H_{\frac{1}{2},+}^2 + H_{\frac{1}{2},0}^2 + H_{-\frac{1}{2},-}^2 + H_{-\frac{1}{2},0}^2) + \frac{2m_l^2}{3q^2} \left[H_{\frac{1}{2},+,-}^{T^2} + H_{\frac{1}{2},0,t}^{T^2} + H_{\frac{1}{2},+,0}^{T^2} + H_{\frac{1}{2},+,t}^{T^2} \right. \\
&\quad \left. + H_{-\frac{1}{2},+,-}^{T^2} + H_{-\frac{1}{2},0,t}^{T^2} + H_{-\frac{1}{2},0,-}^{T^2} + H_{-\frac{1}{2},-,t}^{T^2} + 2(H_{\frac{1}{2},+,-}^T H_{\frac{1}{2},0,t}^T + H_{\frac{1}{2},+,0}^T H_{\frac{1}{2},+,t}^T \right. \\
&\quad \left. + H_{-\frac{1}{2},+,-}^T H_{-\frac{1}{2},0,t}^T + H_{-\frac{1}{2},0,-}^T H_{-\frac{1}{2},-,t}^T) \right] \\
&\quad + \frac{8m_l}{3\sqrt{q^2}} (H_{\frac{1}{2},0} H_{\frac{1}{2},+,-}^T + H_{\frac{1}{2},0} H_{\frac{1}{2},0,t}^T + H_{\frac{1}{2},+} H_{\frac{1}{2},+,0}^T + H_{\frac{1}{2},+} H_{\frac{1}{2},+,t}^T \\
&\quad + H_{-\frac{1}{2},0} H_{-\frac{1}{2},+,-}^T + H_{-\frac{1}{2},0} H_{-\frac{1}{2},0,t}^T + H_{-\frac{1}{2},-} H_{-\frac{1}{2},0,-}^T + H_{-\frac{1}{2},-} H_{-\frac{1}{2},-,t}^T). \tag{A1}
\end{aligned}$$

Appendix B: Form factors relations

The relation between various form factors are given as [51, 52]

$$\begin{aligned}
f_0 &= f_1 + \frac{q^2}{M_{\Lambda_b} - m_\Lambda} f_3, & f_+ &= f_1 - \frac{q^2}{M_{\Lambda_b} + m_\Lambda} f_2, & f_\perp &= f_1 - (M_{\Lambda_b} + m_\Lambda) f_2, \\
g_0 &= g_1 - \frac{q^2}{M_{\Lambda_b} + m_\Lambda} g_3, & g_+ &= g_1 + \frac{q^2}{M_{\Lambda_b} - m_\Lambda} g_2, & g_\perp &= g_1 + (M_{\Lambda_b} - m_\Lambda) g_2, \\
h_+ &= f_2^T - \frac{M_{\Lambda_b} + m_\Lambda}{q^2} f_1^T, & h_\perp &= f_2^T - \frac{1}{M_{\Lambda_b} + m_\Lambda} f_1^T, \\
\tilde{h}_+ &= g_2^T + \frac{M_{\Lambda_b} - m_\Lambda}{q^2} g_1^T, & \tilde{h}_\perp &= g_2^T + \frac{1}{M_{\Lambda_b} - m_\Lambda} g_1^T,
\end{aligned} \tag{B1}$$

with

$$\begin{aligned}
f_2^T &= f_T - f_T^S q^2, & f_1^T &= (f_T^V + f_T^S (M_{B_1} - M_{B_2})) q^2, & f_1^T &= -\frac{q^2}{M_{B_1} - M_{B_2}} f_3^T, \\
g_2^T &= g_T - g_T^S q^2, & g_1^T &= (g_T^V + g_T^S (M_{B_1} + M_{B_2})) q^2, & g_1^T &= \frac{q^2}{M_{B_1} + M_{B_2}} g_3^T.
\end{aligned} \tag{B2}$$

-
- [1] J. P. Lees et al. (BaBar), Phys. Rev. Lett. **109**, 101802 (2012), 1205.5442.
 - [2] J. P. Lees et al. (BaBar), Phys. Rev. **D88**, 072012 (2013), 1303.0571.
 - [3] M. Huschle et al. (Belle), Phys. Rev. **D92**, 072014 (2015), 1507.03233.
 - [4] A. Abdesselam et al. (Belle), in *Proceedings, 51st Rencontres de Moriond on Electroweak Interactions and Unified Theories: La Thuile, Italy, March 12-19, 2016* (2016), 1603.06711, URL <http://inspirehep.net/record/1431982/files/arXiv:1603.06711.pdf>.
 - [5] R. Aaij et al. (LHCb), Phys. Rev. Lett. **115**, 111803 (2015), [Erratum: Phys. Rev. Lett.115,no.15,159901(2015)], 1506.08614.
 - [6] Y. Amhis et al. (Heavy Flavor Averaging Group), Eur. Phys. J. **C77**, 895 (2017), updated results and plots available at <https://hflav.web.cern.ch>, 1612.07233.
 - [7] R. Aaij et al. (LHCb), Phys. Rev. Lett. **120**, 121801 (2018), 1711.05623.
 - [8] R. Aaij et al. (LHCb), Phys. Rev. Lett. **113**, 151601 (2014), 1406.6482.
 - [9] R. Aaij et al. (LHCb), JHEP **08**, 055 (2017), 1705.05802.
 - [10] C. Bobeth, G. Hiller, and G. Piranishvili, JHEP **12**, 040 (2007), 0709.4174.
 - [11] B. Capdevila, A. Crivellin, S. Descotes-Genon, J. Matias, and J. Virto, JHEP **01**, 093 (2018), 1704.05340.

- [12] H. Na, C. M. Bouchard, G. P. Lepage, C. Monahan, and J. Shigemitsu (HPQCD), Phys. Rev. **D92**, 054510 (2015), [Erratum: Phys. Rev.D93,no.11,119906(2016)], 1505.03925.
- [13] S. Fajfer, J. F. Kamenik, and I. Nisandzic, Phys. Rev. **D85**, 094025 (2012), 1203.2654.
- [14] S. Fajfer, J. F. Kamenik, I. Nisandzic, and J. Zupan, Phys. Rev. Lett. **109**, 161801 (2012), 1206.1872.
- [15] W.-F. Wang, Y.-Y. Fan, and Z.-J. Xiao, Chin. Phys. **C37**, 093102 (2013), 1212.5903.
- [16] M. A. Ivanov, J. G. Korner, and P. Santorelli, Phys. Rev. **D71**, 094006 (2005), [Erratum: Phys. Rev.D75,019901(2007)], hep-ph/0501051.
- [17] C. Patrignani et al. (Particle Data Group), Chin. Phys. **C40**, 100001 (2016).
- [18] R. Aaij et al. (LHCb), Phys. Rev. **D85**, 032008 (2012), 1111.2357.
- [19] R. Aaij et al. (LHCb), JHEP **08**, 143 (2014), 1405.6842.
- [20] R. Aaij et al. (LHCb), Nature Phys. **11**, 743 (2015), 1504.01568.
- [21] M. Fiore, in *Proceedings, Meeting of the APS Division of Particles and Fields (DPF 2015): Ann Arbor, Michigan, USA, 4-8 Aug 2015* (2015), 1511.00105.
- [22] Y. K. Hsiao and C. Q. Geng, Eur. Phys. J. **C77**, 714 (2017), 1705.00948.
- [23] R. M. Woloshyn, PoS **Hadron2013**, 203 (2013).
- [24] W. Wu, Master's thesis, Mississippi U. (2015), 1505.03418, URL <http://search.proquest.com/docview/1697862095>.
- [25] S. Shivashankara, W. Wu, and A. Datta, Phys. Rev. **D91**, 115003 (2015), 1502.07230.
- [26] T. Gutsche, M. A. Ivanov, J. G. Korner, V. E. Lyubovitskij, and P. Santorelli, Phys. Rev. **D93**, 034008 (2016), 1512.02168.
- [27] T. Gutsche, M. A. Ivanov, J. G. Krner, V. E. Lyubovitskij, P. Santorelli, and N. Haby, Phys. Rev. **D91**, 074001 (2015), [Erratum: Phys. Rev.D91,no.11,119907(2015)], 1502.04864.
- [28] W. Detmold, C. Lehner, and S. Meinel, Phys. Rev. **D92**, 034503 (2015), 1503.01421.
- [29] R. Dutta, Phys. Rev. **D93**, 054003 (2016), 1512.04034.
- [30] M. Pervin, W. Roberts, and S. Capstick, Phys. Rev. **C72**, 035201 (2005), nucl-th/0503030.
- [31] R. N. Faustov and V. O. Galkin, Eur. Phys. J. **C76**, 628 (2016), 1610.00957.
- [32] A. Datta, S. Kamali, S. Meinel, and A. Rashed, JHEP **08**, 131 (2017), 1702.02243.
- [33] X.-Q. Li, Y.-D. Yang, and X. Zhang, JHEP **02**, 068 (2017), 1611.01635.
- [34] E. Di Salvo, F. Fontanelli, and Z. J. Ajaltouni (2018), 1804.05592.
- [35] F. U. Bernlochner, Z. Ligeti, D. J. Robinson, and W. L. Sutcliffe (2018), 1808.09464.

- [36] T. Bhattacharya, V. Cirigliano, S. D. Cohen, A. Filipuzzi, M. Gonzalez-Alonso, M. L. Graesser, R. Gupta, and H.-W. Lin, Phys. Rev. **D85**, 054512 (2012), 1110.6448.
- [37] V. Cirigliano, J. Jenkins, and M. Gonzalez-Alonso, Nucl. Phys. **B830**, 95 (2010), 0908.1754.
- [38] P. Biancofiore, P. Colangelo, and F. De Fazio, Phys. Rev. **D87**, 074010 (2013), 1302.1042.
- [39] S. Aoki et al., Eur. Phys. J. **C74**, 2890 (2014), 1310.8555.
- [40] T.-W. Chiu, T.-H. Hsieh, C.-H. Huang, and K. Ogawa (TWQCD), Phys. Lett. **B651**, 171 (2007), 0705.2797.
- [41] A. G. Akeroyd and C.-H. Chen, Phys. Rev. **D96**, 075011 (2017), 1708.04072.
- [42] Y. Sakaki, M. Tanaka, A. Tayduganov, and R. Watanabe, Phys. Rev. **D88**, 094012 (2013), 1309.0301.
- [43] M. Tanaka and R. Watanabe, Phys. Rev. **D87**, 034028 (2013), 1212.1878.
- [44] A. Khodjamirian, T. Mannel, N. Offen, and Y. M. Wang, Phys. Rev. **D83**, 094031 (2011), 1103.2655.
- [45] C. Bourrely, I. Caprini, and L. Lellouch, Phys. Rev. **D79**, 013008 (2009), [Erratum: Phys. Rev.D82,099902(2010)], 0807.2722.
- [46] C. G. Boyd, B. Grinstein, and R. F. Lebed, Phys. Rev. Lett. **74**, 4603 (1995), hep-ph/9412324.
- [47] C. G. Boyd, B. Grinstein, and R. F. Lebed, Phys. Lett. **B353**, 306 (1995), hep-ph/9504235.
- [48] M. A. Ivanov, J. G. Krner, and C.-T. Tran, Phys. Rev. **D95**, 036021 (2017), 1701.02937.
- [49] C.-T. Tran, M. A. Ivanov, J. G. Krner, and P. Santorelli, Phys. Rev. **D97**, 054014 (2018), 1801.06927.
- [50] M. A. Ivanov, J. G. Krner, and C.-T. Tran, Phys. Rev. **D94**, 094028 (2016), 1607.02932.
- [51] T. Feldmann and M. W. Y. Yip, Phys. Rev. **D85**, 014035 (2012), [Erratum: Phys. Rev.D86,079901(2012)], 1111.1844.
- [52] C.-H. Chen and C. Q. Geng, Phys. Rev. **D64**, 074001 (2001), hep-ph/0106193.